

The effect of azathioprine on bone health

Stephanie Morgan

BSc (Hons)

A thesis submitted in partial fulfilment of
the requirements of Edinburgh Napier
University, for the award of Master by
Research

October 2019

Acknowledgment

I would like to express my deepest appreciation for my supervisor's Katherine Staines and Craig Stevens. From day one Katherine was wonderful, taking me from being nervous and shy about standing up and talking to audiences to a more confident researcher who can appreciate asking for advice. She was there for me throughout this experience and I greatly appreciate her patience and close attention to detail. Craig was always there to support me through any issues I was having whether it be in the lab or in my writing. He helped build my confidence in speaking and answering questions in front of an audience which I will be forever grateful for. I would also like to thank Kirsty Hooper, who without her previous research my study would not have been possible. Kirsty was also very welcoming to me at the beginning of my postgraduate experience which I am very thankful for. I would like to show my appreciation to Elspeth Milne for the work she carried out on the colon pathology which was extremely valuable to this project. Also, for his help with our mouse study I would like to thank Colin Farquharson whose assistance was invaluable to this study. To the members of my research group, David Hughes, Jasmine Samvelyan and Raquel Lopera-Burgueno I would like to thank you for your support and kindness. Lastly, I would like to thank my family and friends for their moral support throughout this study.

Abstract

Individuals with inflammatory bowel disease (IBD) often present with poor bone health and have increased risk of osteoporotic bone fractures. The development of targeted therapies for this bone loss requires a better understanding of the underlying cellular mechanisms. Azathioprine is a commonly used drug for IBD management and has been shown to induce autophagy within the colon. However, its mechanisms of action, in particular its effects on the skeleton, are not yet fully understood. Herein, the dextran sulphate sodium (DSS) model of colitis was induced in mice to examine the effects of azathioprine treatment on bone health. Micro-computed tomography assessment of vehicle-treated DSS mice revealed a worsened trabecular bone architecture compared to vehicle-treated control mice. The azathioprine treated mice were found to have decreased bone architecture when treated with the drug alone without the presence of colitis, and there was a partial protection provided to the DSS-treated animals with azathioprine treatment. However, when combined with DSS, azathioprine provides partial protection against damage to bone architecture. Histological analysis revealed that azathioprine treatment induced autophagy in the bone. This indicates that azathioprine reduces bone health in an *in vivo* model of IBD. This therefore suggests that azathioprine treatment may have a deleterious effect on IBD patients who may already be at increased risk of osteoporotic bone fractures and thus will inform on future treatment strategies for patient stratification.

Publications

Original peer-reviewed papers

Morgan S., Hooper K.M., Milne E.M., Farquharson C., Stevens C., Staines K.A. 2019
The effect of azathioprine on bone health in an *in vivo* model of IBD. *Disease models & mechanisms*. In preparation

Presented abstracts

Morgan S., Hooper K., Milne E., Farquharson C., Stevens C., Staines K.A. Azathioprine protects against poor bone health in mice with DSS induced inflammatory bowel disease. Bone Research Society, Winchester (2018).

Morgan S., Hooper K., Milne E., Farquharson C., Stevens C., Staines K.A. Azathioprine protects against poor bone health in mice with DSS induced inflammatory bowel disease. ENU research conference (2018).

Morgan S., Hooper K., Milne E., Farquharson C., Stevens C., Staines K.A. Azathioprine protects against poor bone health in mice with DSS induced inflammatory bowel disease. EMG winter conference (2018). Award: poster prize winner

List of Abbreviations

6-MP	6-mercaptopurine
ANOVA	One-way analysis of variance
ATG	Autophagy related
ATG16	Autophagy-related 16
Atp	Adenosine tri-Phosphate
BCP	Biphasic calcium phosphate
Bglap	Osteocalcin
BMD	Bone mineral density
Ca²⁺	Calcium ions
CD	Crohn's Disease
cDNA	Complimentary DNA
CO₂	Carbon Dioxide
Col1a1	Collagen type 1 alpha 1
Ctx	Fragments of C-terminal telopeptides of Col1a1
DAB	Diaminobenzidine
dH₂O	Distilled H ₂ O
DMSO	Dimethyl sulfoxide
DNA	Deoxyribonucleic acid
DSS	Dextran sulphate sodium

ECM	Extracellular matrix
EDTA	Ethylenediaminetetraacetic acid
FBS	Foetal bovine serum
GWAS	Genome-wide association studies
H&E	Haematoxylin and eosin
H₂O	Water
H₂O₂	Hydrogen peroxide
HA	Hydroxyapatite
IBD	Inflammatory Bowel Disease
IgG	Immunoglobulin G
IL	Interleukin
IRGM	Immunity-related GTPase family M
Micro-CT	Micro-computed tomography
MSCs	Mesenchymal stromal cells
mTOR	Mechanistic target of rapamycin
NCP	Non-collagenous protein
NFκB	Nuclear factor-kappa B
NOD2	Nucleotide-binding oligomerization domain-containing protein 2
NSAID	Nonsteroidal anti-inflammatory drug
P1NP	N-terminal propeptide of Collagen alpha-1(I) chain

PBS	Phosphate Buffered Saline
PBST	Phosphate Buffered Saline with Tween
PFA	Paraformaldehyde
Pi	Inorganic phosphate
Postn	Periostin
PVDF	Polyvinylidene fluoride
RANK	Receptor activator of nuclear factor kappa-B
RANKL	Receptor for activation of nuclear factor kappa B ligand
RNA	Ribonucleic acid
RT- qPCR	Real-time Quantitative polymerase chain reaction
SNP	Single nucleotide polymorphism
TGF-β	Transforming growth factor-beta
TLR	Toll-like receptor
TNF	Tumour necrosis factor
TRAF	Tumour necrosis factor receptor-associated factor
TRAP	Tartrate-resistant acid phosphatase
UC	Ulcerative Colitis
α-MEM	α -modified essential medium
βGP	Beta-glycerophosphate

Table of Contents

Chapter 1: Introduction	1
1.1. Inflammatory bowel disease	2
1.1.1. Pathogenesis of IBD	3
1.2. Autophagy	6
1.2.1. Autophagy signalling pathways	8
1.3. Current treatments of IBD	10
1.3.1. Aminosalicylates	10
1.3.2. Corticosteroids	10
1.3.3. Immunomodulators	11
1.3.4. Biologic agents	11
1.3.5. Thiopurines	11
1.4. Bone	12
1.4.1. Bone mineralisation	14
1.4.2. Bone modelling and remodelling	15
1.4.2.1. Osteoblasts	15
1.4.2.2. Osteoclasts	17
1.4.2.3. Osteocytes	17
1.4.2.4. Osteoporosis	18
1.5. Inflammatory bowel disease and bone	19
1.6. Autophagy and bone	21
1.6.1. Autophagy in osteoblasts	21

1.6.2. Autophagy in osteocytes	22
1.6.3. Autophagy in osteoclasts	23
1.6.4. Autophagy in osteoporosis	24
1.7. Aims	25
Chapter 2: Materials and methods	26
2.1. Animal study	27
2.2. Micro computed tomography (μ CT)	28
2.3. Histological studies	29
2.3.1. Tissue processing	29
2.3.2. Immunohistochemistry	30
2.3.3. Goldners trichrome staining	30
2.3.4. Haematoxylin and eosin staining	31
2.3.5. Pathological analysis of the colon	31
2.4. ELISA	31
2.5. Cell culture	32
2.6. Cell treatment	33
2.7. RNA methods	33
2.7.1. Extraction of RNA from cells	33
2.7.2. Reverse transcription	34
2.7.3. Real-time polymerase chain reaction (RT-qPCR)	34

2.8. Protein methods	35
2.8.1. Protein extraction	35
2.8.2. DC protein assay	35
2.8.3 Western blotting	36
2.8.4 Stripping PVDF membrane for additional western blotting	37
2.9. Statistical analysis	37
Chapter 3: Effect of IBD treatment on bone health in an in vivo model of IBD	38
3.1. Introduction	39
3.2. Materials and method	40
3.2.1. Animal model	40
3.2.2. Colon phenotyping	40
3.2.3. Bone phenotyping	41
3.3. Results	41
3.3.1. The effect of DSS treatment on body weight and longitudinal bone growth of mice	41
3.3.2. Colon pathology in DSS-treated mice	43
3.3.3. Bone phenotype of DSS treated mice	45
3.3.4. ELISA	50
3.4. Discussion	51
Chapter 4: Effect of azathioprine on osteoblast health	54

4.1. Introduction	55
4.2. Materials and methods	56
4.2.1. Tissue processing and immunohistochemistry	56
4.2.2. Cell culture and treatment	56
4.2.3. RNA analysis of MC3T3 cells	57
4.2.4. Protein extraction and western blot	57
4.3. Results	58
4.3.1. Autophagy induction in azathioprine treated mice	58
4.3.2. Effect of azathioprine on osteoblast health	61
4.4. Discussion	65
Chapter 5: Final discussion	68
5.1. General discussion	69
5.2. Future work	72
References	75
Appendix	87

Chapter 1

Introduction

1.1. Inflammatory bowel disease

Inflammatory bowel disease (IBD) is the umbrella name given to two similar conditions that affect the gastrointestinal system: Ulcerative Colitis (UC) and Crohn's disease (CD). Both diseases are characterised by the inflammation of the gastrointestinal system (Pithadia & Jain, 2011). CD can affect any part of the gastrointestinal tract and can cause transmural inflammation. In contrast, UC causes mucosal inflammation and is limited to the colon (Zhang & Li, 2014). A recent review by NHS England revealed that the prevalence of IBD was 1 in every 250 people which results in a total cost of £720 million a year in costs to the NHS (NHS England, 2014).

IBD patients suffer from periods of relapse and remission. During relapse, patients often suffer from symptoms such as nausea, fever, abdominal pain, fatigue and weight loss (Henderson et al., 2012). Fatigue continues to play a large role in patients day to day life even when in remission (Czuber-Dochan et al., 2013). In addition to day to day symptoms, IBD can also result in secondary conditions such as colon cancer, arthritis and osteoporotic bone loss (Diefenbach & Breuer, 2006). It is this secondary osteoporotic bone loss in IBD which is the focus of this thesis.

In CD, the most affected area of the gastrointestinal tract is the terminal ileum. In more than 90% of patients, the disease is located in three main sites: large bowel, isolated small bowel disease and the combined involvement of the large and small bowel (Langholz, 2010). CD results in a granulomatous inflammatory response, a specific form of chronic inflammation which is characterised by the collection of epithelioid cells, multinucleated cells and macrophages. The development of this inflammatory response depends on a complex immune reaction leading to necrosis and fibrosis (Freeman, 2014). CD can be diagnosed at any age, but onset is most frequently in the second decade of life. Any early onset of CD is often very extensive and is characterised by rapid disease progression

(Marcuzzi. et al., 2013). Patients with CD often suffer from strictures of the bowel or fistula formation - ulceration that extends through the intestinal wall allowing connections between different body parts. Fistula formation can extend into the bladder, the vagina, the skin (often following surgery) and most commonly around the anal area (Crohn's and Colitis UK, 2013).

The inflammation in UC typically involves only the innermost lining or mucosa, causing continuous areas of ulceration with no sections of normal tissue (Head. & Jurenka., 2003). There a number of varieties of UC: disease involving only the distal area of the colon is known as ulcerative proctitis, UC from the descending colon and lower is termed distal colitis and any disease involving the whole colon is referred to as pancolitis (Kucharzik et al., 2006). Like CD, UC can be diagnosed at any age but usually occurs before the age of 30. Because early symptoms are similar to those of irritable bowel syndrome, initial diagnosis can be challenging (Head. & Jurenka., 2003).

1.1.1. Pathogenesis of IBD

While the pathogenesis of IBD is not entirely understood, it is thought that the genetic susceptibility of an individual, the intestinal microbial flora, external environment and immune responses are all involved in the development and progression of IBD (Knights et al., 2013).

Several environmental factors play an important role in the pathogenesis of IBD. Factors including smoking, diet, gut bacteria, and drugs are all considered to increase IBD risk (Diefenbach & Breuer, 2006). Smoking increases the risk of relapse frequency in CD in addition to increasing the need for surgery. Contrary to the effect of smoking on CD, studies have confirmed that it can have a protective effect on the development of UC (Danese et al., 2004). A number of links have also been made between different dietary factors and IBD development. It has been observed that a diet high in red meat, margarine

and cheese, along with the decreased consumption of fruit and fibre appear to increase the risk of IBD development (Maconi et al., 2010). Drugs such as antibiotics and nonsteroidal anti-inflammatory drugs (NSAIDs) are two of the main classes of drugs that effect the development of IBD. NSAIDs have been associated with increased risk of CD and UC when used for a prolonged time (Zhang & Li, 2014). Antibiotics have also been found to increase the risk of IBD as a result of their effect on the microbiome. This is especially common in children diagnosed with IBD as it has been found that infants with IBD were often found to have used antibiotics in their first year of life (Shaw et al., 2010).

The intestinal immune system is responsible for defending against pathogens and the entry of intestinal microbes. An imbalance in this process is considered to predispose to IBD (Abraham & Medzhitov, 2011). Patients with IBD have altered immune mechanisms of the epithelial layer. It is thought that IBD occurs when a breakdown in the epithelial barrier exposes immune cells to bacteria and luminal antigens (Shih et al., 2008). The breakdown of the epithelial layer combined with a genetic predisposition is thought to be required to trigger IBD. An upregulation of NOD2 in epithelial cells may also cause a reduction in the hosts ability to eliminate pathogenic microbes and this can result in chronic inflammation (Baumgart & Carding, 2007).

Over the last few decades, advances in genetic testing has allowed for the completion of many genome-wide association studies (GWAS) which has allowed the identification of single nucleotide polymorphisms (SNPs) associated with IBD. GWAS have identified more than 200 IBD associated susceptible loci (Nishida et al., 2017). Some of these susceptibility genes are known to be involved in mediating the responses of the host to gut microbiota (Nishida et al., 2017). Over 28 genes have been linked with both forms of IBD whereas some loci have been found to be specific to CD or UC which may provide a new way to look at the common pathogenesis of UC and CD (Zhang & Li, 2014). Some of the CD-related genes found include Nucleotide-binding oligomerization domain-

containing protein 2 (NOD2), autophagy-related 16 (ATG16) and immunity-related GTPase family M (IRGM), as is discussed further in section 1.5 (Kohr et al., 2011).

The association between NOD2 and IBD was made in 2001 and it was found that homozygous mutation of NOD2 gene increases the risk of developing IBD 20 to 40 fold (Hooper et al., 2017). NOD2 is highly expressed in macrophages, dendritic cells and in epithelial cells of the intestine. It is activated by N-acetyl muramyl dipeptide and binds to receptor interacting serine-threonine kinase 2 (RIP2, RIPK2) which results in the activation of the NF- κ B pathway (Kaser et al., 2010). The variant of NOD2 associated with IBD does not bind to RIP2 which decreases the activation of the NF- κ B pathway.

ATG16L1 is located on chromosome 2 at 2q37.1 and encodes a protein that is involved in autophagosome formation. ATG16L1 was first identified in 2007 as a susceptible gene for IBD (Hampe et al., 2007). A SNP shown by the marker rs2241880, that encodes a threonine to alanine substitution (T300A) was linked to CD susceptibility (Hampe et al., 2007). A mouse model with ATG16L1 deficiency showed Paneth cell dysfunction along with increased expression of pro-inflammatory cytokines and lipid metabolism genes, similar to the Paneth cell phenotype of CD patients (Marcuzzi. et al., 2013). Paneth cells are secretory epithelial cells of the small intestine that are key effectors of the innate mucosal defence (McSorley & Bevins, 2013).

The IRGM gene is found on chromosome 5q33.1 and was reported as being an IBD susceptible gene in 2007 (Parkes et al., 2007). In humans, IRGM is formed from 181 amino acids and is found in the small and large intestine and expressed by lymphocytes. IRGM is known to be involved in virus-induced autophagy, phagosome maturation and bacterial killing (Jo, 2013). IRGM encodes a GTP-binding protein that is involved in the regulation of autophagy activating in response to intracellular pathogens (Rufini et al., 2015). It has been found that IRGM regulates a complex that includes NOD2 and

ATG16L1 which is necessary for the activation of autophagy. These genes are involved in bacteria-immune interactions and indicate impaired autophagy of invasive gut microbes (Kohr et al., 2011).

1.2. Autophagy

Autophagy protects cells from several pathological stresses and also plays a crucial role during development and in the maintenance of cellular homeostasis (Iriarte Rodríguez et al., 2015). There are three different autophagic routes: macroautophagy, microautophagy and chaperone-mediated autophagy (CMA) (Choi et al., 2013). Microautophagy is the non-selective lysosomal degradative process which involves the direct engulfment of cytoplasmic material at a boundary membrane by autophagic tubes which are responsible for the mediation of vesicles scission into the lumen (Jian & Bao, 2012). CMA is a selective form of autophagy through which specific cytosolic proteins are transported individually across the lysosomal membrane for degradation (Orenstein & Cuervo, 2010). The most common form of autophagy is microautophagy, herein referred to as autophagy, and this is an essential self-eating process that allows the degradation of intracellular components such as organelles, foreign bodies and soluble proteins (Yu et al., 2017).

One of the main features of the autophagy pathway (Fig. 1.1) is the formation of endomembranous organelles called autophagosomes. A number of factors such Beclin 1 and autophagy related (ATG) proteins are key regulators driving the formation of the autophagic isolation membrane, also referred to as the phagophore (Deretic et al., 2013). The phagophore is derived from phosphatidylinositol 3-phosphate (PI3P)-positive domains of the endoplasmic reticulum known as omegasomes. The Golgi, mitochondria and other membrane derived organelles also contribute to the formation of the phagophore (Klionsky & Codogno, 2013). The essential genes required for the formation of the autophagosome are referred to as the core machinery genes (Kang et al., 2018).

They are classed into three groups: transmembrane proteins (example ATG9), the phosphoinositide-3-kinase (PI3K) complex and ubiquitin-like protein conjugation systems (ATG12 and ATG8/LC3).

Next, a complex is formed on the phagophore between ATG16L1 and ATG5-12 which then lipidates LC3, the mammalian homologue of Atg8 found on both the outer and inner membranes of the autophagosome. At the same time, the phagophore elongates to engulf the cytoplasm or organelle destined to be degraded thus forming an autophagosome, a unique double-membrane organelle (Iida et al., 2017). There are two forms of LC3- LC3I and LC3II. LC3 is cleaved by Atg4 to liberate a C-terminal glycine needed for the conjugation to phospholipids upon the induction of autophagy. This binding forms LC3II and is essential for the extension and closure of the phagophore to form the autophagosomes (Iii et al., 2010; Glick et al., 2010). LC3II is present throughout the membrane to help select the material to be engulfed by the autophagosome and assists with the membrane fusion (Glick et al., 2010; Itakura & Mizushima, 2011). LC3 is a dependable way to monitor autophagy activity as the amount of LC3-II, the conjugated form of LC3 correlates with the number of autophagosomes (Kuma et al., 2007). Bafilomycin can be used to inhibit autophagy through the inhibition of the acidification of the lysosome that stops the cargo from being degraded (Vinod et al., 2014). Bafilomycin was also found to block the fusion of the autophagosome to the lysosome (Yamamoto et al., 1998). Because of this bafilomycin can be used to measure autophagy levels as it results in the build-up of autophagy marker LC3-II (Figure 1.1).

The intracellular protein degradation mechanism is then triggered when the autophagosome matures and fuses with lysosomes to degrade its contents. The first step of autophagosome fusion is when the outer membrane fuses with a single lysosome membrane. The fusion is complete when the inner autophagosomal membrane is degraded by lysosomal hydrolases and the contents are exposed to the lumen of the

Chapter 1: Introduction

lysosome (Yu et al., 2017). The amino acids and other products of degradation are exported back into the cytoplasm by lysosomal permeases and transporters. Here they can be used for building macromolecules and for metabolism (Glick et al., 2010).

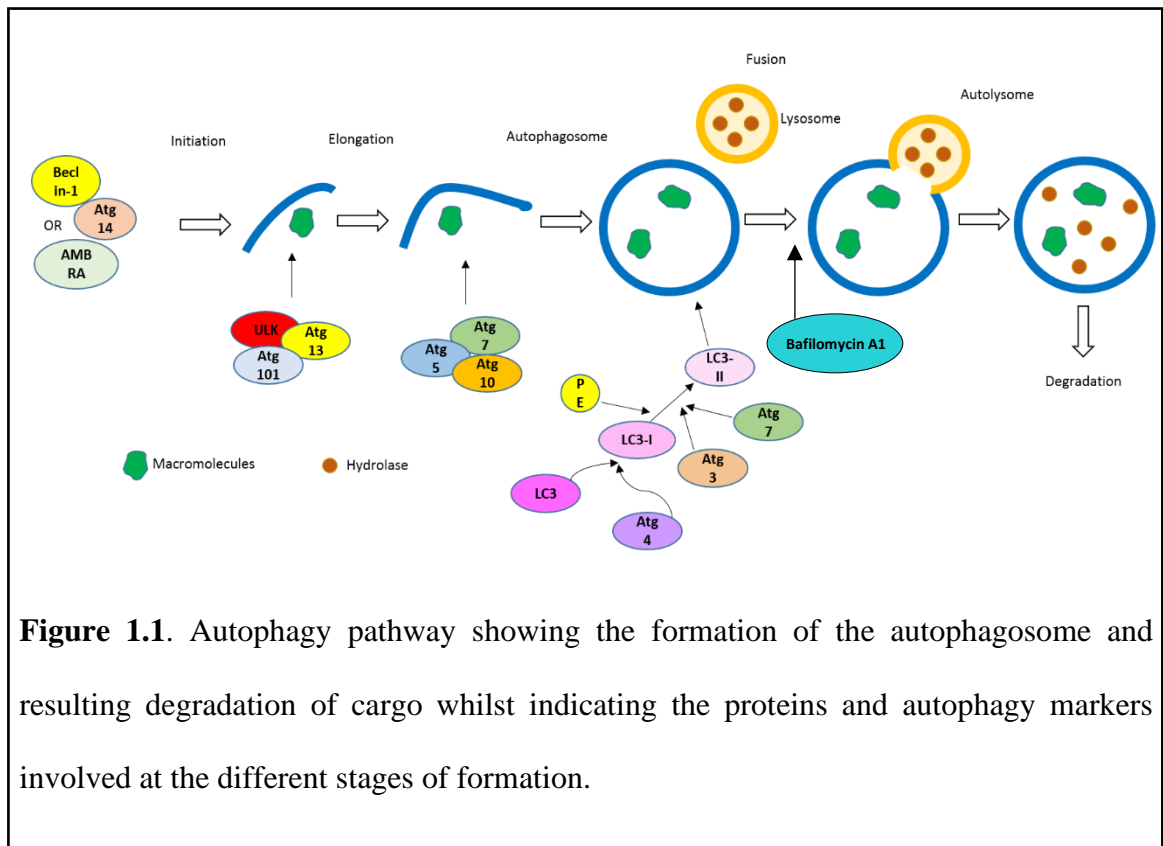


Figure 1.1. Autophagy pathway showing the formation of the autophagosome and resulting degradation of cargo whilst indicating the proteins and autophagy markers involved at the different stages of formation.

1.2.1. Autophagy signalling pathways

Autophagy is triggered by a number of inductive signals that begin the formation of the phagophore (Hurley & Schulman, 2014). Two of the systems that control the autophagy process are the mTOR-ULK1 and the beclin-1 pathway (Lilienbaum, 2013).

mTOR or mechanistic target of rapamycin, phosphorylates and inactivates Atg13 and ULKs under nutrient rich conditions. The inhibition of mTOR can be caused by starvation or treatment with rapamycin, resulting in the activation of ULK1, ULK2 and phosphorylate Atg13 which is essential for autophagy (He & Klionsky, 2009). There are two forms of mTOR, mTOR complex 1 (mTORC1) and mTOR complex 2 (mTORC2).

mTORC1 is involved in anabolic processes such as translation, lipid synthesis and tRNA production. It is also involved in the regulation of energy through the repression of autophagy when conditions are nutrient sufficient (Mckee-muir & Russell, 2017). However, mTORC2 is not sensitive to nutrient sufficiency and is responsible for the downstream regulation of pathways including PI3K-AKT and cytoskeletal organisation (Gaubitz et al., 2016). P62 is a scaffold protein that helps to regulate ubiquitin-mediated downstream signalling from multiple receptors including toll-like receptors and TNF receptors (Ciuffa et al., 2015). P62 been found to be a regulator of mTORC1 activation to regulate the nutrient sensing response (Duran et al., 2016). During autophagy, p62 is constantly degraded due to its binding with LC3 which keeps the expression of p62 low in non-stressed cells. P62 is upregulated when autophagy is disrupted which makes it a good marker for autophagy activity (Duran et al., 2016).

The autophagosome nucleation during autophagy requires a complex which contains Atg6 or its mammalian homolog Beclin1. Beclin1 recruits phosphatidylinositol (PI) 3-kinase which is used to generate PI3P (Qian et al., 2017). PI3P recruits proteins to modulate intracellular trafficking and the formation of the autophagosome (Kim et al., 2012). The process started with the beclin1 results in the development of the autophagosome membranes.

1.3. Current treatments of IBD

Despite substantial research and further development in IBD treatment, patients are not often able to return to their former quality of life. There are a number of different treatment options including thiopurines and corticosteroid. However, apart from the mildest of cases, a lot of treatment is through immunosuppression, often leading to surgery (Diefenbach & Breuer, 2006). IBD drugs are often used in combination to limit side effects and make the treatment more effective for the patient.

1.3.1 Aminosalicylates

Aminosalicylates such as sulphasalazine and mesalazins are anti-inflammatory treatments that are used to induce and maintain remission in patients with UC however clinical trials have not shown them to be as effective in the treatment of CD (Hanauer, 2004). Many mechanisms of action have been described including the scavenging of damaging reactive oxygen species (ROS), inhibition of leukocyte motility, interference with nuclear factor-kappa B (NFκB) and the inhibition of IL-1 synthesis (Desreumaux & Ghosh, 2006). It was recognised that 5-aminosalicylic acid (5-ASA) is the active moiety in UC has allowed the development of numerous medication formulas including sulfasalazine (sulfapyridine bound to 5-ASA) (Hanauer, 2004).

1.3.2. Corticosteroids

One of the first methods of treatment to induce remission for IBD is through the use of corticosteroids which downregulate proinflammatory cytokines (Iida et al., 2017). Although the use of corticosteroids has been seen to reduce remission in 84% of patients, long term treatment is often not an option due to severe adverse effects and the steroid dependency seen in 30-45% of patients (Markowitz, 2008). Long term effects include bone loss, venous thromboembolism and poor wound healing (Waljee et al., 2016). The use of corticosteroids in IBD reduce inflammatory mediators by binding with the glucocorticoid receptor expressed by immune cells. The binding results in the expression of proinflammatory transcription factors such as NFκB and the apoptosis of target inflammatory cells (Lichtenstein, 2006).

1.3.3. Immunomodulators

Methotrexate, cyclosporin and tacrolimus are forms of immunomodulatory drugs that are mainly used to maintain remission in severe forms of IBD (Pithadia & Jain, 2011). Methotrexate works by inhibiting RNA and DNA synthesis in dividing cells whereas

cyclosporin and tacrolimus block the production of IL-2 that results in a reduction of T cell activity (Dieren et al., 2006; Markowitz, 2008). Treatment with immunomodulators can have several side effects including nausea, bone marrow suppression and ulcerative stomatitis (Markowitz, 2008). Concentration of thiopurine metabolites are closely monitored in patients as high levels can result in hepatotoxicity and myelosuppression (Hooper et al., 2017).

1.3.4. Biologic agents

Biologic agents such as infliximab are anti-inflammatory drugs that work by binding to both soluble and membrane bound TNF in both CD and UC (Markowitz, 2008). Therapy with infliximab is used for both the induction and maintenance of remission due to the removal of TNF from the circulation and death of lymphocytes and monocytes which are essential to the initiation of inflammation (Hyams et al., 2007; Moss & Farrell, 2006). In addition, infliximab is used to reduce the number of rectovaginal fistulas and maintaining fistula closure in patients with fistulising CD (Lichtenstein, 2006).

1.3.5 Thiopurines

Thiopurines have been proven effective in IBD in maintaining remission, monitoring steroid withdrawal and fistula closure (Dubinsky, 2004). Examples of thiopurines are Azathioprine and Mercaptopurine which are taken by as many as 60% of patients (Cosnes et al., 2005). Both drugs have a slow onset of action but are able to maintain remission in moderate to severe cases of IBD (Gisbert et al., 2011). Although the use of mercaptopurine has a steroid sparing effect during remission the side effects of the drugs may outweigh the benefits of thiopurines. Side effects of thiopurine use can be severe with patients suffering from nausea, pancreatitis and recurrent infections. There is also a risk of developing lymphoma as a result of treatment (Dubinsky, 2004).

Azathioprine is converted to 6-mercaptopurine (6-MP) in the intestinal wall, liver and red blood cells via glutathione. The drug is broken down into thiopurine metabolites, methylmercaptopurine nucleotides and thioguanine nucleotides. The nucleotides cause the inhibition of DNA, RNA and protein synthesis resulting in immunosuppression (Stocco et al., 2015). It was observed that autophagy may play a protective role against the adverse effects caused by thiopurine treatment as autophagy was seen to be induced in hepatocytes upon treatment with azathioprine (Hooper et al., 2017). The mechanism of action of azathioprine is known to involve both apoptosis and autophagy and azathioprine has previously been found to induce autophagy in peripheral blood mononuclear cells and colorectal cancer cells (Hooper et al., 2019; Chaabane & Appell, 2016).

1.4. Bone

The skeleton is a highly intricate and complex organ that is adapted to suit its function, being both strong yet light allowing it to withstand loading whilst allowing movement and flexibility to prevent fractures (Farquharson & Staines, 2011). The human adult skeleton is made up of 206 separate bones which are supported by cartilage, muscles and tendons. The skeleton contains 99% of the total calcium in the human body and is specialised for the protection of vital organs, mineral homeostasis and the regulation of metabolism (Brandi, 2009). Bone is made up of both organic and inorganic material and a combination of organic collagen and hydroxyapatite mineral results in a structure that is strong and resistant to fracture (Staines et al., 2012).

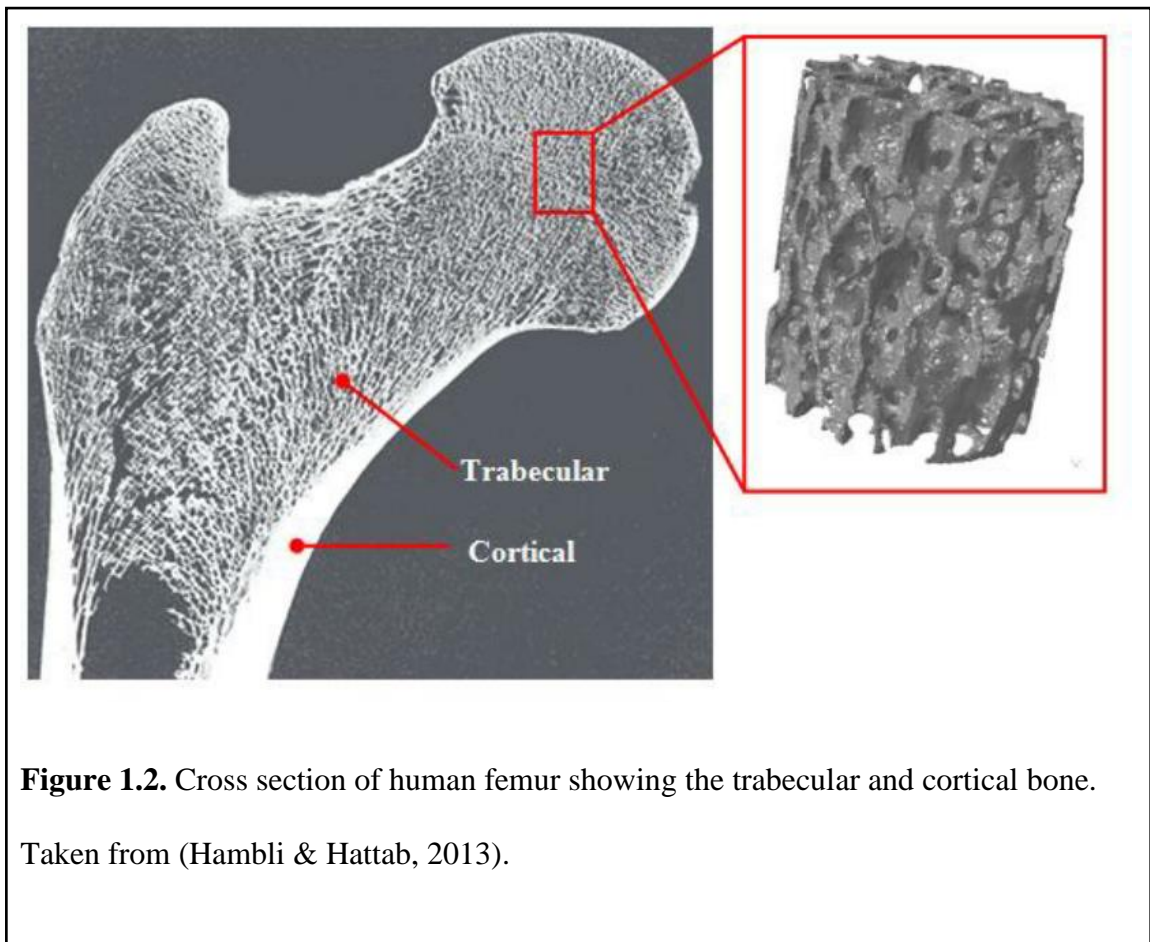
Bone forms by two distinct mechanisms, both of which involve a number of different biochemical and morphological processes. The development and formation of flat bones, such as the skull and clavicle, happens as result of a process called intramembranous ossification which involves the direct differentiation of embryonic mesenchymal cells

into osteoblasts (see section 1.2.2.1) (Mackie et al., 2011). In contrast long bones such as the femur are formed by endochondral ossification which involves a cartilage anlagen being replaced by bone tissue (Mackie et al., 2011). Long bones consist of the epiphyses and metaphyses at each end, and the diaphysis in the middle. Located in the metaphysis is a developmental cartilaginous region termed the growth plate. The growth plate is responsible for postnatal bone growth and consists of chondrocytes arranged in columns surrounded by their extracellular matrix (ECM). The chondrocytes of the growth plate sit in distinct cellular zones of maturation and undergo defined stages of differentiation to enable longitudinal bone growth (Mackie et al., 2011). This continues until sexual maturity has been reached at which point the growth plate fuses through the formation of bone bridges and is replaced by an epiphyseal line (Shapiro, 2008).

The skeleton consists of two different types of bone tissue, cortical bone and trabecular bone. The cortical bone makes up around 80% of the skeleton and is found in the shafts of long bones and the outer surfaces of flat bones (Brandi, 2009). Cortical bone is well organised into osteon building units which have resident osteocytes (see section 1.2.2.3). These osteocytes run through a canaliculi network which connects the osteocytes with osteoblasts and osteoclasts on the bone surface (Sommerfeldt & Rubin, 2001). The trabecular bone is found mainly at the end of long bones and in the inner parts of flat bones (Brandi, 2009). The trabecular bone consists of an open lattice network with abundant haemopoietic tissue and fat, thereby reducing the weight of bone. Compared to the cortical bone, trabecular bone has a high turnover rate and can adapt to loading in multiple directions (Sommerfeldt & Rubin, 2001). The proportions of the two different types of bone tissue vary depending on the skeletal site (Brandi, 2009) (Fig. 1.2).

1.4.1. Bone mineralisation

Bone mineralisation begins with membrane bound matrix vesicles (MV) which are formed by both osteoblasts and chondrocytes. These vesicles provide a protective environment for calcium ions (Ca^{2+}) and inorganic phosphate (Pi) to accumulate (Staines et al., 2014). High concentrations of Ca^{2+} and Pi leads to their precipitation into hydroxyapatite crystals. These crystals then increase in size and pass through the MV membrane where they are deposited onto collagen fibrils (Anderson, 2003). This process is regulated by several factors such as alkaline phosphatase and non-collagenous proteins (NCPs) (Olszta et al., 2007).



1.4.2. Bone modelling and remodelling

Bone modelling happens as a result of bone formation and resorption and causes changes to the size and shape to allow the bone to adapt to any changes in mechanical loading. On the other hand, bone remodelling replaces old bone with new bone without any changes in the overall bone mass (Raggatt & Partridge, 2010). Bone is constantly remodelled throughout the entire lifetime which allows the complete skeleton to be replaced every 10 years (Weinstein & Manolagas, 2000). There are three types of cells involved in the bone remodelling process; osteoblasts which are responsible for bone formation, osteoclasts which are involved in bone resorption and osteocytes which are responsible for forming a network between other cells in the bone and as such, play a key role in the regulation of bone remodelling (Manolagas, 2000).

1.4.2.1. Osteoblasts

Osteoblasts are specialised bone forming cells which are differentiated from mesenchymal stromal cells (MSC)s (Jung et al., 2008). Osteoblasts account for 4-6% of the total bone cells and are responsible for the secretion of the osteoid which mineralises to offer strength to the skeleton (Florencio-Silva et al., 2015). Osteoblasts are characterised by prominent Golgi apparatus, rough endoplasmic reticulum as well as a number of secretory vesicles (Florencio-Silva et al., 2015).

The differentiation of osteoblasts involves several factors including transforming growth factor-beta (TGF- β), bone morphogenic protein (BMP) and transcription factors such as Runx2, osterix and β -catenin (Chen et al., 2012; Komori, 2006). Once the process is activated by expression of Runx2, the MSCs undergo a three-stage differentiation. Firstly, the cells continue to proliferate and express collagen type I, osteopontin and TGF- β . They then begin to differentiate while maturing the ECM with collagen type I and alkaline phosphatase. Then matrix mineralisation then occurs due to the abundance of osteocalcin

which promotes the deposition of mineral substance. At this stage the osteoblast forms its characteristic cuboidal shape (Rutkovskiy et al., 2016).

There are many known markers of the osteoblast phenotype including osteocalcin (*Bglap*), periostin (*Postn*) and collagen type 1 (*Coll1a1*) (Florencio-Silva et al., 2015; Garnero, 2009). Osteocalcin is a non-collagenous, vitamin K-dependant protein that is produced by osteoblasts (Razzaque, 2011). It is coded for by the *Bglap* gene in mice and provides a non-invasive marker of osteoblast activity and bone formation. The osteocalcin protein contains three residues of the amino acid gamma-carbo-xyglutamic acid (Gla). In the company of calcium, the Gla residues facilitate the binding of osteocalcin to HA and deposition in the bone matrix (Razzaque, 2011). Periostin is an extracellular matrix protein which is coded for by the *Postn* gene and is expressed in osteoblasts (Cobo et al., 2016). Periostin null mice have been found to have undersized bones, a restricted trabecular network and often suffer from dwarfism (Rios et al., 2005). Loss of malfunction has been found to result in altered trabecular and cortical bone microarchitecture and overall lower bone density (Chapurlat & Confavreux, 2016). Collagen type 1 is encoded by *Coll1a1* in mice, is secreted by osteoblasts and provides the scaffold for the deposition of HA crystals in bone mineralisation (Van Dijk et al., 2010; Nudelman et al., 2010). Genetic polymorphisms of *Coll1a1* is associated with low bone mineral density and high fracture risk in humans (Kostik et al., 2013).

Once the osteoblast has matured and has deposited the bone ECM, it either differentiates into an osteocyte by a process known as osteocytogenesis (see section 1.2.2.3) or undergoes apoptosis (Dallas & Bonewald, 2010).

1.4.2.2. Osteoclasts

Osteoclasts are a part of the monocyte/macrophage lineage and are formed when multiple mononuclear cells fuse together in the bone marrow. The receptor activator of nuclear

factor kappa-B (RANK) is found on osteoclast precursor cells and contains a tumour necrosis factor (TNF) receptor-associated factor (TRAF). The ligand for RANK receptor (RANKL) is expressed on the surface of mesenchymal cells, lymphocytes and osteoblasts. The binding of RANK to RANKL induces osteoclast differentiation. RANK controls the initiation of downstream molecules through the use of TRAF that results in osteoclast differentiation (Kim & Kim, 2016). The signals produced from the downstream molecules are involved in the stimulation of tartrate-resistant acid phosphatase (TRAP)- which is a recognised marker of osteoclast differentiation (Kim & Kim, 2016). Osteoclasts are responsible for the resorption of bone a process which is closely regulated to prevent the development of different bone disorders (Väänänen & Laitala-Leinonen, 2008). Osteoclasts adhere to the bone matrix through the formation of a ruffled border, and then secrete acid and lytic enzymes that cause degradation.

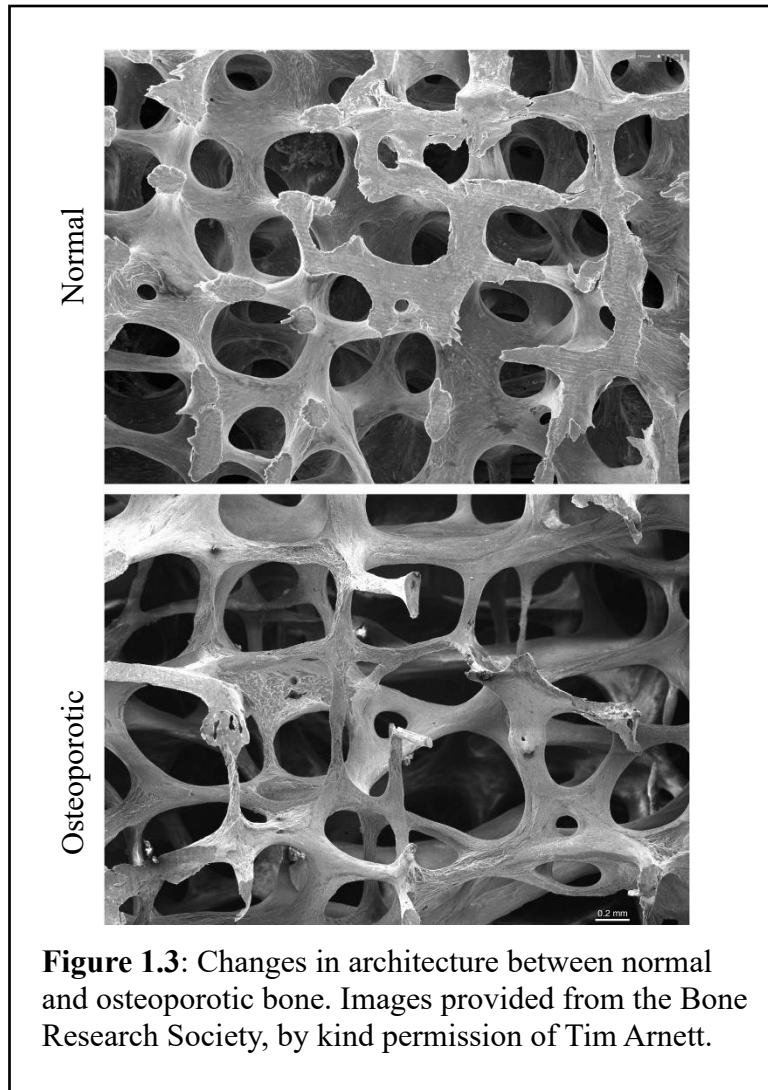
1.4.2.3. Osteocytes

Osteocytes comprise of 90-95% of all bone cells and have a lifespan of up to 25 years (Franz-Odenaal et al., 2006). Osteocytes are located within lacunae embedded in mineralised bone ECM and have a unique dendritic morphology. Osteocytes are surrounded by a canalicular fluid which delivers nutrients and oxygen from the circulation. This fluid carries hormones and provides access to therapeutic drugs (Compton & Lee, 2014). Osteocytes are derived from the differentiation of osteoblasts and this process occurs in four stages, termed osteocytogenesis: osteoid-osteocyte, preosteocyte, young osteocyte and mature osteocyte (Franz-Odenaal et al., 2006). One of the first things to happen in the embedding cell is the development of dendritic processes. These dendrites form towards the mineralising front and then extend further to either the bone surface or vascular space enabling the osteocyte to connect with other osteocytes, osteoblasts and osteoclasts. The osteocyte is thought to carry out many functions concurrently, including mechanotransduction, calcium and phosphate

regulation and the regulation of bone remodelling (Bonewald, 2011). A marker that osteocytes have become mature is the production of the Wnt inhibitor sclerostin which acts as a negative regulator for bone formation (Bonewald, 2011). More recently it has been shown that osteocytes regulate bone remodelling through the expression of RANKL (Xiong et al., 2012; Nakashima et al., 2011).

1.4.2.4. Osteoporosis

Osteoporosis is a skeletal disorder that is characterised by low bone mass (Figure 1.3) with an increase in bone fragility thus making individuals with osteoporosis susceptible to fracture (Sambrook & Cooper, 2010). This is due to an imbalance in the bone remodelling process, in favour of increased bone resorption. Osteoporosis has been associated as secondary to a number of gastrointestinal conditions including IBD and it is estimated that more than 35% of patients with IBD will develop osteoporosis (Ali et al., 2010; Bianchi, 2010).



1.5. Inflammatory bowel disease and bone

Both forms of IBD, UC and CD, are associated with a significant reduction in bone mass in both adults and children. CD often affects bone mass more severely than UC especially in growing children, most likely because CD affects linear growth and normal development of the skeletal muscle mass more so than UC (Sylvester & Vella, 2016). The occurrence of osteopenia in IBD is 32-36% and osteoporosis is 7-15%. Indeed patients with IBD are 40% more at risk of bone fracture than a healthy individual (Ali et al., 2010; Agrawal et al., 2011).

Bone loss in IBD is thought to be caused by two main factors, malabsorption and inflammation (Bianchi, 2010). Intestinal absorption of key determinants of bone health – e.g. Ca^{2+} and vitamin D – is often altered in IBD due to the reduction of intestinal mucosa (Bianchi, 2010). In addition, patients with IBD often reduce or avoid milk and other dairy foods therefore limiting the calcium available for absorption. The loss of albumin and immunoglobulins is well documented in IBD and since vitamin D is carried in the plasma by vitamin-D binding globulin the loss of vitamin D is common in IBD patients (Bianchi, 2010).

In IBD, the immune response leads to the production of proinflammatory cytokines such as interleukin (IL) -2 and tumour necrosis factor (TNF). In mononuclear cells, (NF κ B) regulates the transcription of IL -1, 6 and 8. It also regulates proinflammatory genes such as chemokines and TNF- α (Ali et al., 2010). Many proinflammatory osteoclast activators including TNF- α and IL -1,6,11 and 17 are upregulated in patients with IBD, thereby providing a potential mechanism in favour of increased osteoclast function. Variations in the IL-6 and IL-1 receptor genes have also been connected with the clinical course of IBD and the degree of bone loss (Schulte et al., 2000). Chronic inflammation is mediated by T-cells which can produce RANKL that can trigger bone loss through the activation of osteoclasts (Clowes et al., 2005).

A model of IBD has been utilised in a number of studies using dextran sulphate sodium (DSS) to induce colitis in mice. The DSS treatment induces colitis by causing a toxic effect on intestinal cells. This leads to a fissure in the mucosal barrier which exposes the contents to luminal antigens which results in inflammation (Hamdani et al., 2008). DSS produces similar effects to UC such as mucosal inflammation and focal crypt lesions and also displays features of CD such as ulceration and submucosal inflammation (Harris et al., 2009). The treatment with DSS has been previously linked to a reduction in bone mass and formation and therefore makes an effective model to observe bone loss in IBD.

1.6. Autophagy and bone

1.6.1. Autophagy in osteoblasts

Osteoblasts are derived from MSCs and evidence suggests that autophagy is crucial for these MSC progenitors. It has been shown that the induction of autophagy could produce a survival response against oxidative stress in MSCs from the bone marrow (Song et al., 2014). An accumulation of autophagic vacuoles is observed in undifferentiated MSCs, and these are consumed during early differentiation into osteoblasts, indicating that they are used as a source of energy (Nuschke et al., 2014). Further, the differentiation of MSCs is also reported to be controlled by AMPK through early mTOR inhibition-mediated autophagy (Pierrefite-Carle et al., 2015).

Osteoblasts are responsible for bone formation through the secretion of bone ECM and the ensuing ECM mineralisation. Intracellular mineralisation could be mediated by autophagy through autophagic vacuoles acting as vehicles for HA crystal secretion (Pierrefite-Carle et al., 2015). Further, it has been shown that autophagy is involved in major aspects of osteoblast ECM mineralisation (Nollet et al., 2014). When autophagy is inhibited, osteoblast ECM mineralisation has been found to decrease which could suggest that autophagic vacuoles could serve to secrete HA crystals to the extracellular space (Nollet et al., 2014). The disruption of NBR1, an autophagic receptor for the degradation of ubiquitinated substrates, has an effect on the activity and differentiation of osteoblasts (Waters et al., 2009). NBR1 manages this by interacting with LC3 protein members through its LC3- interacting region and by binding with the targets through the ubiquitin-like modifier activating enzyme (UBA) domain (Shapiro et al., 2014). In a mouse model where the NBR1 protein is inhibited, high bone mass and increased bone mineral density was observed in older mice as a result of the increased osteoblast activity (Whitehouse et al., 2010).

Certain families of transcription factors are known to have roles in autophagy and assist in the control of osteoblast survival and function. One family, FOXO transcription factors, plays key roles in cell growth and proliferation, energy homeostasis and glucose metabolism (Demontis & Perrimon, 2010). The activation of FOXO induces autophagy through the direct binding to the promotor region of the target genes. The genetic deletion of FOXO transcription factors in osteoblasts increases apoptosis and oxidative stress which mimics the aging process (Almeida, 2011). Because of the role of autophagy in protection against oxidative stress it is thought that the induction of autophagy may mediate the role of FOXO in the maintenance of bone homeostasis.

The skeletal adaptive response to mechanical loading is mediated by osteoblasts and osteocytes. They do this by causing a cascade of biochemical and structural changes in response to mechanical forces. It has been observed that autophagy is sensitive to changes in mechanical pressure in mammalian cells (King et al., 2011). Certain pressures, around the control of 0.2kPa are required to cause changes in osteoblasts whilst also inducing autophagy (Kanzaki et al., 2002). Once again, it can be observed that autophagy plays a key role in bone homeostasis.

1.6.2. Autophagy in osteocytes

Osteocytes are terminally differentiated osteoblasts and are found embedded within the mineralised bone. Due to their long life and location, osteocytes are known to be dependent on autophagy for their survival (Zahm et al., 2011). Autophagy is also induced in osteocytes in response to hypoxia and starvation, both which often occur in their usual environment. In pre-osteocyte-like murine cells (MLO-A5), autophagy was found to be upregulated in response to calcium stress and hypoxia inducible factor 1, α subunit (HIF1A) which indicates that low oxygen pressure serves as a positive regulator of autophagy (Zahm et al., 2011). The induction of autophagy in osteocytes was shown to

offer protection in response to cellular stress caused by glucocorticoid treatment and thus prolonging the survival of the osteocytes (Xia et al., 2010). An age-related decline in autophagic activity has also been described in rat osteocytes with a decrease in LC3 and Beclin-1 observed whilst the expression of p62 and levels of apoptosis were increased (Chen et al., 2014).

1.6.3. Autophagy in osteoclasts

Osteoclasts are multinucleated cells that are formed by the joining of multiple myeloid precursors. This is triggered by RANKL and M-CSF, and monocyte chemoattractant protein-1 (MCP-1) is also known to induce this differentiation process (Kim et al., 2006). It was observed MCP-1 differentiation is mediated by Beclin-1 upregulation and autophagy (Wang et al., 2011). TRAF3, which is involved in the suppression of RANKL-induced osteoclast formation, is degraded by autophagy as a result of RANKL in osteoclast precursors from bone marrow (Xiu et al., 2014).

Further, it has been shown that some of the ATGs such as Atg5, Atg7 and LC3 are required for the osteoclast ruffled border generation, bone resorption and secretory activity. Atg5 attracts LC3-II to the ruffled border and this induces the fusion of the osteoclast plasma membrane with lysosomes which is needed in the resorption of bone (DeSelm et al., 2011). Osteoclast activity was further associated with the conversion of LC3-I to LC3-II. However, the knockdown of LC3 did not affect TRAP-positive multinucleated osteoclasts cell formation, but suppressed the osteoclast bone-resorbing capacity (Chung et al., 2012).

1.6.4. Autophagy in osteoporosis

As evidenced above, autophagy plays a vital role in the maintenance of bone homeostasis and therefore any alterations in this pathway are related to the development of

osteoporosis (Florencio-Silva et al., 2017a). Besides the loss of sex hormones, increased oxidative stress is recognised as a major factor in the development of osteoporosis which suggests that autophagy could play a critical role in age-related bone loss (Almeida & Brien, 2013).

The effect of the mTOR pathway on skeletal growth has recently been explored and it was found that rapamycin, an inhibitor of mTOR, can reduce the growth of body weight, alter the growth of long bones, cause changes to the structure of the growth plate and affect fracture healing (Shen et al., 2018). mTOR signalling inhibitors have been used in the treatment of osteosarcoma suggesting that the inhibition of mTOR may also have a positive impact on bone (Moriceau et al., 2010). It has been suggested that the interaction of mTOR signalling with other pathways such as NF- κ B or RANKL may also be a potential mechanism of action for osteoporosis and thus could be a promising therapeutic target (Shen et al., 2018).

Further, treatment of male mice with high levels of glucocorticoids reduced the percentage of LC3 positive osteoblasts resulting in the a loss of cell viability and subsequent osteoporotic bone loss (Yao et al., 2016). However, the administration of an antibody against sclerostin, an inhibitor of bone formation, prevented glucocorticoid-induced bone loss by increasing autophagy and maintaining the health of osteoblasts. Together this therefore suggests that increases in autophagy may protect against bone loss in osteoporosis. However, the role of autophagy in IBD-related osteoporosis has yet to be established.

1.7. Aims

The aim of this study is to investigate the effects of the IBD drug azathioprine on bone health. It will test the hypothesis that: *azathioprine stimulates autophagy in the skeleton in IBD and thus provides protection against IBD-related osteoporosis.*

To address this hypothesis, this study will examine the following aims:

1) Assess the effects of azathioprine on bone health in an *in vivo* model of IBD. This will test the hypothesis that: *azathioprine has a detrimental effect on bone health in an in vivo model.*

2) Determine whether azathioprine modulates autophagy in the skeleton. By determining the stimulation of autophagy by azathioprine, it will test the hypothesis that: *azathioprine induces autophagy in the skeleton in IBD therefore providing a defence against osteoporosis resulting from IBD.*

Results from this study may help to prevent unwanted side effects of azathioprine treatment on bone health in IBD patients and both the economic and social burden of this disease.

Chapter 2

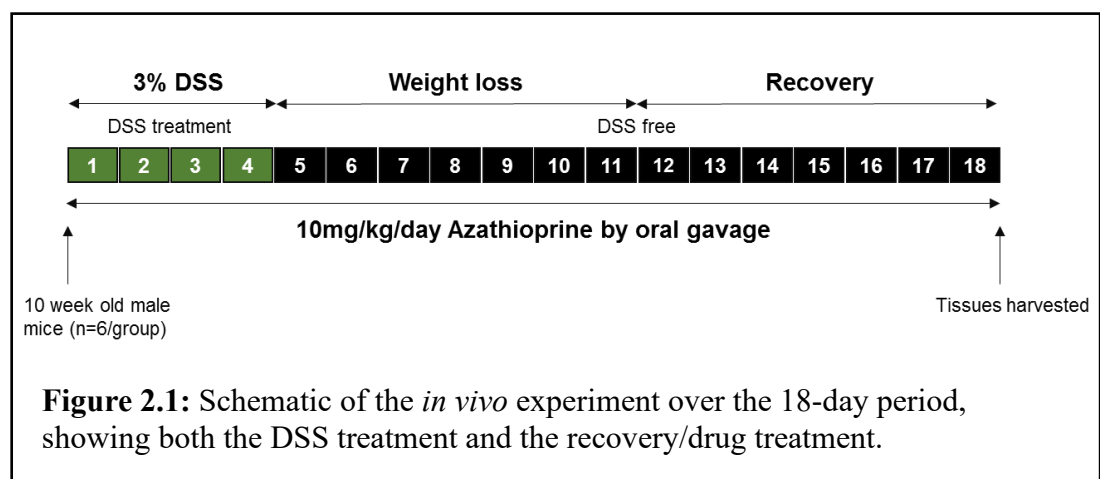
Materials and

methods

Chapter 2: Materials and Methods

2.1. Animal study

An IBD *in vivo* murine model, previously established by the research team, was used to investigate the effects of azathioprine on IBD-related bone health (Dobie et al., 2017). Ten-week old male mice (n=6/group) (Charles River, UK) were treated with 3% dextran sulphate sodium (DSS) (MP Biomedical, UK) in their drinking water for 4 days to induce colitis (Fig. 2.1). Following this they were given a 14-day recovery period where they were given normal water. Mice were treated using an oral gavage throughout the experiment with 10 mg/kg/day of azathioprine or a vehicle control (n=6/group). Control mice (non-DSS treated), receiving either the vehicle control or azathioprine were treated with normal tap water for the duration of the study. Overall, there were 4 treatment groups utilised in this study, DSS treatment with a vehicle control, DSS treatment with azathioprine, water with vehicle control and water with azathioprine. The health of the mice was monitored throughout the experiment by taking the weight of each mouse daily and closely monitoring the health of their coats and behaviours. Mice were kept in polypropylene cages, with light/dark 12-hr cycles, at $21 \pm 2^\circ\text{C}$, and fed ad libitum with maintenance diet (Special Diet Services, Witham, UK). All experimental protocols were approved by Roslin Institute's Animal Users Committee and the animals were maintained in accordance with UK Home Office guidelines for the care and use of laboratory animals.



Chapter 2: Materials and Methods

After the 14-day recovery period the mice were culled and colon and bone tissues were collected. The right tibia from each mouse was dissected and frozen in dH₂O at -20°C until required. The right femur and colon were fixed in 4% paraformaldehyde for 24 hours at 4°C before being stored in 70% ethanol. The left femur had the ends removed, the bone marrow spun out and then the bone was snap frozen in liquid nitrogen and stored at -80°C until required. Blood was collected upon death and spun at 1000g for 15 minutes. The serum was aliquoted and stored at -80°C until required.

2.2. Micro computed tomography (μCT)

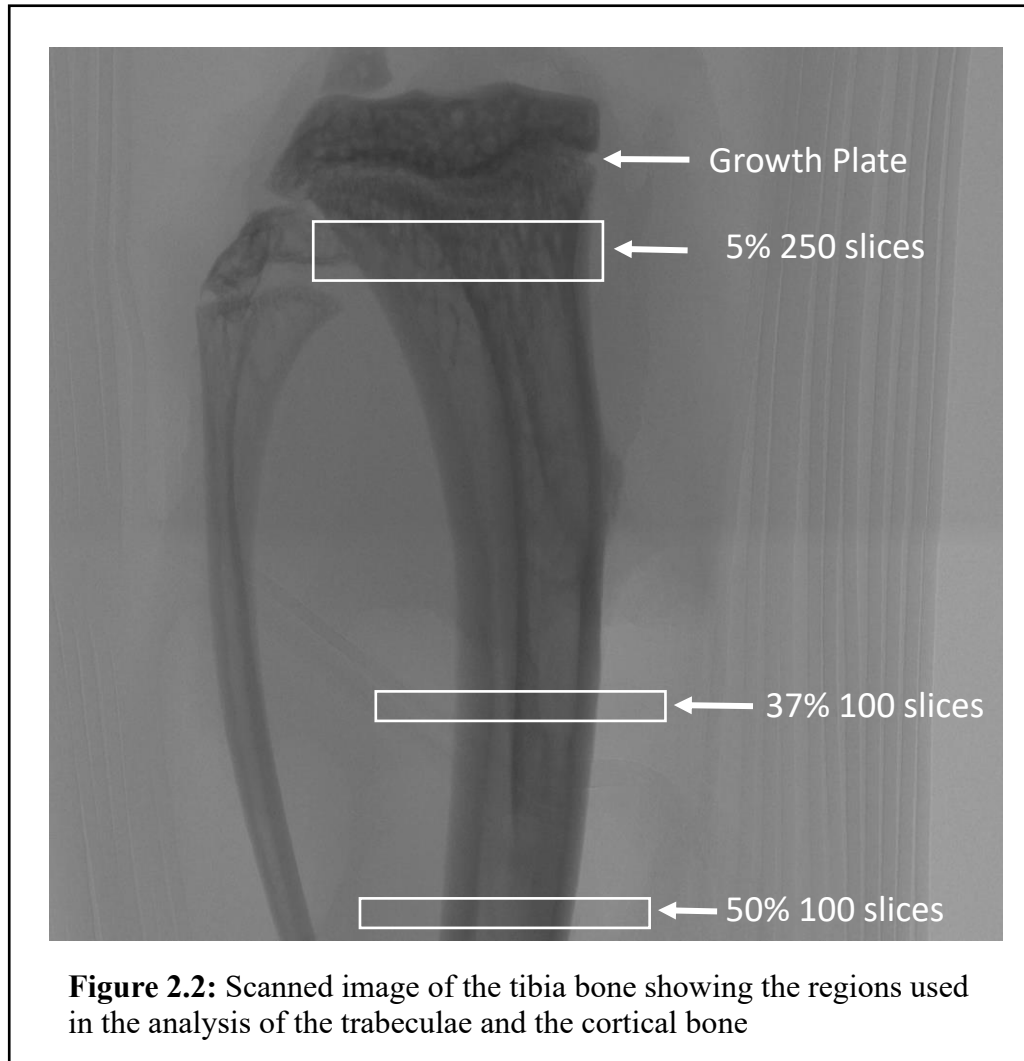
The right tibia bone from each mouse was scanned with an 1172 X-Ray microCT (Skyscan, Belgium) at 5 μm resolution (60kV, 167μA, 0.5 mm aluminium filter, 0.6° rotation angle, two frame averaging, and exposure time 1650). The projection images were reconstructed using NRecon software version 1.6.9.4 (Skyscan, Belgium).

To determine any changes in the bone microarchitecture, the trabeculae in comparative regions of interest were examined. The bottom of the growth plate was located as a reference on each of the scanned bones. A section of 250 slices was then analysed, at 5% of the total bone length beneath the growth plate reference point (Fig. 2.2). Trabeculae were isolated using CtAn and using BatMan (Skyscan), changes in trabecular parameters were examined: Bone Volume/Tissue Volume (BV/TV, %), Trabeculae thickness (Tb.Th mm), Trabeculae pattern factor (Tb.Pf, 1/mm), Number of Trabeculae (Tb.N, 1/mm), Bone mineral density (BMD).

Following the analysis of changes in the trabeculae, changes in the cortical bone were also examined. Two sections of 100 slices were selected at 37% and 50% from the top of the bone (Fig. 2.2). The cortical bone was highlighted using CtAn and BatMan (Skyscan) and changes in the cortical parameters were analysed: Bone Volume/Tissue Volume

Chapter 2: Materials and Methods

(BV/TV, %), Tissue Area (T.Ar), Tissue Perimeter (T.Pm), Bone Area (B.Ar) and Bone Perimeter (B.Pm), Bone mineral density (BMD).



2.3. Histological studies

2.3.1. Tissue processing

Following tissue dissection and fixation (section 2.3), the left tibia from all mice was decalcified in 10% ethylenediaminetetraacetic acid (EDTA) at 4°C for approximately 6 weeks. Tissue processing, paraffin embedding, and sectioning (5 μm) of the tibia and the colon were done following routine procedures.

2.3.2 Immunohistochemistry

A Vectastain ABC kit (Vector Laboratories, Peterborough, UK) was used for the immunohistochemical analysis of the samples according to the instructions from the manufacturer. The samples were first de-waxed in xylene and then rehydrated through a series of alcohol dilutions from absolute alcohol to distilled H₂O. Antigen retrieval was carried out using 10 mM citrate buffer (pH 6) for 90 minutes at 70°C in the oven. After 3 x 5-minute washes in PBS, any endogenous peroxidase activity was blocked by using 0.3% H₂O₂ for 30 minutes at room temperature. Following a further 3 x 5 minute PBS washes the sections were blocked using the normal blocking buffer for 30 minutes at room temperature. The sections were then treated with the primary antibody (see Table 2.2) diluted in the blocking buffer. The controls were treated with an equal concentration of rabbit immunoglobulin G (IgG). All samples were left at 4°C overnight.

Following the incubation with the primary antibody the samples were washed for 3 x 5 minutes in PBS before being incubated in the biotinylated secondary antibody for 30 minutes at room temperature. The sections were then washed again for 3 x 5 minutes in PBS before being incubated in the ABC reagent for another 30 minutes at room temperature. Before staining the samples were washed in PBS. The sections were then stained using diaminobenzidine (DAB) solution for 5 minutes. The samples were then rinsed in tap water and counterstained with haematoxylin before being dehydrated through ethanol to xylene. The sections were then mounted onto microscope slides using DePex and left to dry before microscopic analysis. The immunohistochemical expression was quantified using ImageJ software.

2.3.3. Goldners trichrome staining

As previously described, the sections were dewaxed and rehydrated to water before being stained in wiegert's haematoxylin for 10 minutes. The slides were then washed for 10

Chapter 2: Materials and Methods

minutes before being immersed in Ponceau Acid Fuchsin. The sections were washed in 1% acetic acid (2 x 5 min) then placed in phosphomolybdic Acid-Orange G solution. The sections were washed again in acetic acid (2 x 5min) and placed in the light green stock solution. The slides were rinsed in dH₂O before being mounted using DePex and left to dry before microscopic analysis

2.3.4. Haematoxylin and eosin (H&E) staining

The tibia sections were dewaxed and rehydrated in xylene through ethanol before being stained in haematoxylin for 8 minutes. The sections were then washed in running tap water for 10 minutes before being washed in distilled water. The samples were rinsed in 90% alcohol before being counterstained in eosin Y solution for 1 minute. Following counterstaining the slides were dehydrated through alcohol, mounted with DePex and left to dry before microscopic analysis.

2.3.5. Pathological analysis of the colon

Colon pathology was graded blind on sections from all 3 segments of each mouse using an established histological grading scheme by Prof. Elspeth Milne at the University of Edinburgh, following H&E staining (Dieleman et al., 1998). Segments of colon were assessed separately for inflammation. Scores from all five segments were averaged to provide an overall pathology score.

2.4. ELISA

ELISA assays were carried out to test for N-terminal propeptide of Collagen alpha-1(I) chain (P1NP) and Fragments of C-terminal telopeptides of Col1a1 (Ctx). P1NP is used to monitor bone formation and Ctx is a blood biomarker to assess bone resorption.

The Mouse P1NP ELISA Kit and Mouse α -CTx ELISA Kit (AMS Bio., UK) were used to assess blood samples from the DSS mouse model, according to the manufacturer's instructions. Briefly, the standards and samples were plated into 96-well plates before

Chapter 2: Materials and Methods

being incubated at 37°C. For the Ctx, the antibody was added with the sample prior to incubation, whereas the P1NP was added following the incubation. Washes were carried out using wash buffer before TMB substrate was added to each well stimulating a colour change to blue. Stop solution was used causing a yellow colour change before plates were immediately read at 450 nm. The concentration of P1NP/ Ctx in the sample was then calculated.

2.5. Cell culture

Murine MC3T3 osteoblast cells (subclone 14; American Type Culture Collection ATCC, USA) were used throughout this study up to passage 16. The frozen cells were removed from -150°C storage and were thawed in a water bath at 37°C. These were then transferred into a falcon tube with 5 ml of warm medium (α MEM supplemented with 10% foetal bovine serum (FBS) (Sigma Aldrich, Germany) and 5% penicillin/streptomycin (Sigma Aldrich, Germany) (10,000 units/ml penicillin and 10mg/ml streptomycin). Cells were then centrifuged at 136 g for 3 minutes (Hettich Universal 320R) and the supernatant discarded. Cells were resuspended in culture medium and placed in a T175 flask containing 24 ml of culture medium. The cells were left in an incubator set at 37°C with the atmosphere containing 5% CO₂ and left to grow over a period of approximately 2-3 days until a semi-confluent monolayer was formed.

Once the cells had reached 80% confluency, the media was removed from the flask and the cells were wash with distilled water (dH₂O) to remove any remaining FBS in the flask. Following this, 1% trypsin (Sigma Aldrich, Germany) was used to detach the cells from the surface of the flask. The cells were removed from the flask, centrifuged at 136 g for 3 minutes and the supernatant was disposed of. The pellet was resuspended in culture media and the cells were counted using a haemocytometer. The cells were then plated

Chapter 2: Materials and Methods

into 6 well plates at 1×10^5 cells per well and cultured to confluency as described in section 2.2.

2.6. Cell treatment

When the MC3T3 cells had reached 100% confluency (approx. 72hrs) the cells were treated with 50 $\mu\text{g/ml}$ ascorbic acid, to assist in the production of the matrix, and 5 mM beta-glycerophosphate (βGP), to act as a phosphate source for bone mineralisation for a 10-day period. The cells were then treated for 24 hours with 120 μM azathioprine (TOCRIS, UK) or 10 μM rapamycin (Cell Signalling, UK) as the positive control. The negative control was treated with equal concentrations of dimethyl sulfoxide (DMSO) (Sigma Aldrich, Germany). Additionally, an autophagy control (80 nM bafilomycin (Santa Cruz Biotechnology, USA)) was also included with the positive control and the azathioprine test group. Concentrations used were based on previous optimisation experiments from the research group (Singha et al., 2008). The cells were left to incubate for 24 hours before being scrapped for RNA and protein.

2.7. RNA methods

2.7.1. Extraction of RNA from cells

Cells were scraped with 1 ml of cold PBS, centrifuged to form a pellet and stored overnight at -80°C . The RNA was then extracted using the Qiagen RNeasy Kit (Qiagen, Manchester, UK), following the manufacturer's instructions. The cells were first homogenised in the RLT buffer before adding 70% ethanol to allow for the binding of RNA precipitates to the membrane. Buffers and centrifugation were used to remove any contaminants. The RNA was then collected using RNase free water. The amount of RNA collected in $\text{ng}/\mu\text{l}$ was measured using a NanoDrop spectrophotometer (ThermoScientific, Paisley, U.K). The purity of the samples was measured using the ratio of absorbance's at 260/280 wavelengths, and values between 1.8 and 2.1 were used as

Chapter 2: Materials and Methods

optimal. The samples were then diluted using RNase free water and stored at -80 °C for future use.

2.7.2. Reverse transcription

cDNA was obtained from the RNA samples by performing reverse transcription using the Precision nanoscript2 Reverse Transcription kit (Primerdesign, UK). RNA was diluted with RNase free water to equal the lowest concentration among the samples and added to 1 µl Oligo-dT primer. Following heat at 65°C for 5 minutes, the samples were cooled on ice before the addition of the mastermix. The mastermix consists of RNase free water, nanoscript2 enzyme, nanoscript2 reaction buffer and dNTP mix. The samples were further heated at 42°C then 75°C for 30 minutes and diluted with RNase free water to the concentration of 5 ng/µl.

2.7.3. Real-time polymerase chain reaction (RT-qPCR)

The cDNA samples were diluted to 5 ng/µl with RNase free water. A master mix was made up containing 10 µl qPCR master mix with SYBR green (Primerdesign, UK), 4µl of RNase free water and 1 µl of the appropriate primers (see Table 2.1). This was added to 5 µl of diluted cDNA and loaded into a StepOne Real-Time PCR system (ThermoFisher Scientific, UK). The cycle threshold (Ct) values obtained were normalised to *Atp5b* in MC3T3 cell lines and the expression of each gene was calculated using the $2\Delta\text{Ct}$ method (Livak & Schmittgen, 2001).

Chapter 2: Materials and Methods

Gene of Interest	Source	S	Sequence (5'-3')		
BGLAP	Primer Design	Forward	TGCACGAAAGCAAGATGCTG		
		Reverse	GGAGCGTCTGAATAGTCGCC		
Postn	Primer Design	Forward	TTCCTCTCCTGCCCTTATATGC		
		Reverse	CCTGATCCCGACCCCTGAT		
COL1A1	Primer Design	Forward	GCTCCTCTTAGGGGCCACT		
		Reverse	CCACGTCTCACCATTGGGG		
ATP5B (Housekeeping)	Primer Design	Forward	Not disclosed		
		Reverse	Not disclosed		

Table 2.1. Primers used for RT-qPCR analysis.

2.8. Protein methods

2.8.1. Protein extraction

The cell monolayers were washed with PBS before being scraped with 200µl of Radioimmunoprecipitation assay (RIPA) buffer (Thermoscientific, UK), containing protease inhibitor cocktail (Roche, Germany). The cell monolayer was scraped with a sterile cell scraper and transferred to a sterile Eppendorf. The samples were vortexed and stores at -20°C for future analysis. The samples were frozen at -20°C for future use.

2.8.2. DC protein assay

The concentration of protein in each sample was determined using a detergent compatible (DC) assay (Bio-Rad, Watford, UK). The samples were defrosted and vortexed at full speed for 5 minutes. Five microliters of the samples were pipetted in triplicate in a 96-well plate alongside known protein standards. Twenty-five microliters of Bio-Rad DC protein assay Reagent A and 200 µl Bio-Rad DC protein assay Reagent B was added to all samples and standards and the plate was left to incubate for 15 minutes. The absorbance was analysed using a microplate reader at 750 nm. The concentration of each protein samples was determined using the standard curve produced from the standards.

Chapter 2: Materials and Methods

2.8.3. Western blotting

Protein was denatured in a heat block at 70°C for 10 minutes. An equal concentration of protein (30 µg) was loading into a 4-12% Bis Tris protein gel (NuPAGE, Life Tech., UK), which was then loaded into an electrophoresis tank (Xcell Surelock, Invitrogen, UK) containing MES SDS running buffer. To preserve the proteins, antioxidant (NuPAGE, UK) was added to the central chamber and electrophoresis was ran at 200V for 50 minutes.

The protein was transferred to a PVDF (Polyvinylidene fluoride) membrane (Sigma Aldrich, Germany). The PVDF membrane was sandwiched between filter paper and sponges previously soaked in transfer buffer creating a wet transfer. The transfer was carried out on ice at 30V for 70 minutes. The PDVF membrane was blocked in odyssey blocking buffer (Licor, Nebraska, US) for 1 hour at room temperature before being incubated with the appropriate primary antibody (see Table 2.2) overnight at 4 °C.

The primary antibody was washed off in PBST (3 x 10min) at room temperature then incubated for a further 1 hour in the species appropriate secondary antibody (see Table 2.2) diluted in Odyssey buffer. The PDVF membrane was again washed in PBST (3 x 10min). The proteins were then detected using the Licor system (Licor, Nebraska, US).

Antibody	Species	Source	Use	Dilution
LC3	Rabbit	Cell signalling	Western Blot	1 in 1000
LC3	Rabbit	MBL	IHC	1 in 500
p62	Rabbit	Abcam	Western Blot	1 in 1000
p62	Rabbit	Abcam	IHC	1 in 500
Actin	Goat	Santa Cruz Biotech	Western Blot	1 in 1000

Table 2.2. Primary antibodies for western blot and immunohistochemistry

Chapter 2: Materials and Methods

Antibody	Source	Use	Dilution
Goat anti-rabbit	Licor	Western Blot	1 in 1250
Rabbit anti-goat	Licor	Western Blot	1 in 1250
Goat anti-rabbit	Vector Lab	Immunohistochemistry	1 in 10,000

Table 2.3. Secondary antibodies for western blot and immunohistochemistry

2.8.4. Stripping PVDF membrane for additional western blotting

The PVDF membrane was stripped in mild stripping buffer containing glycine and SDS (pH 2.0). The membrane was placed in the stripping buffer for 3 x 7min incubations before being rinsed in distilled water to remove residual buffer. The membrane was then washed in PBST (3 x 5min). The membrane was then re-blocked with odyssey buffer and probed with a different antibody.

2.9. Statistical analysis

Data are presented as mean \pm S.E.M. where $P < 0.05$ was considered to be significant. Data analysis was carried out using GraphPad Prism 6 (GraphPad Software, Inc, USA). Differences between treatment groups were assessed by one-way analysis of variance (ANOVA) for which tests for multiple comparisons were conducted. Tukey and Bonferroni tests were carried out to correct for multiple testing between groups for the *in vivo* results.

Chapter 3

The effects of azathioprine on bone health in an *in* *vivo* model of IBD

3.1. Introduction

Osteoporosis can be a secondary effect to a number of gastrointestinal conditions, including IBD (Ali et al., 2010). Osteoporosis is a metabolic disease of the bone characterised by a reduction in bone mineral density and alterations in bone structure (Bianchi, 2010). Osteoporosis increases the likelihood of bone fracture in the individual. Indeed patients with IBD are 40% more at risk of bone fracture than a healthy individual (Ali et al., 2010).

Bone loss in IBD is thought to be caused by two main factors, malabsorption and inflammation (Bianchi, 2010). Intestinal absorption of key determinants of bone health – e.g. Ca^{2+} and vitamin D - is often altered in IBD due to the reduction of intestinal mucosa (Bianchi, 2010). IBD is also characterised by the chronic release of pro-inflammatory cytokines such as IL-7 and tumour necrosis factor- α (TNF- α) - the increased production of these cytokines can stimulate bone resorption by osteoclasts which therefore leads to excessive bone loss (Bianchi, 2010; Shen, 2004). However, other mechanisms may exist and the development of targeted therapies for this bone loss requires a better understanding of the underlying cellular mechanisms.

Drugs used to treat IBD include steroids, immunosuppressants, aminosalicylates (5-ASAs) and biologic agents. There is an increasing demand to optimise existing medical therapies through patient stratification and personalised medicine (Denson, 2013). It has been previously shown that drugs currently used for IBD can affect autophagy (Hooper et al., 2019), an essential self-eating process that allows the degradation of intracellular components such as organelles, foreign bodies and soluble proteins through the formation and maturation of double membrane vesicles, known as autophagosomes (Yu et al., 2017). Specifically, it was shown that the thiopurine azathioprine is a potent autophagy

Chapter 3: The effects of azathioprine on bone health in an *in vivo* model of IBD

inducer in peripheral blood mononuclear cells (Hooper et al., 2019), however its effects on bone health has yet to be established.

The dextran sulphate sodium (DSS) mouse model is utilised in this study. DSS is thought to induce colitis through a toxic effect on the intestinal cells. It has been found previously that treatment with DSS causes changes in bone structure and can cause bone loss. DSS-induced colitis has been linked with a reduction in bone mass and changed micro architecture. This is caused by suppressed bone formation and increased bone resorption (Hamdani et al., 2008; Dobie et al., 2018).

Therefore, in this chapter, I aimed to establish the effects of azathioprine on bone health by using the (DSS) model of IBD in mice.

3.2. Materials and methods

3.2.1 Animal model

In the DSS model, 24 male 10-week old C57BL/6J WT mice were treated with either 3% DSS-treated or regular water *ad libitum* for 4 days, following which they were given normal tap water for a 14-day recovery period (see section 2.1). Mice were treated daily by oral gavage with 10 mg/kg/day of azathioprine or a vehicle control (n=6/group). After the 14-day recovery period, the mice were culled and blood, colon and bone samples collected (see section 2.1). Control mice (non-DSS treated), receiving the vehicle control or azathioprine were treated with normal tap water for the duration of the study.

3.2.2 Colon phenotyping

Following dissection, the colon of all mice was fixed in 4% paraformaldehyde for 24 hours at 4°C before being stored in 70% ethanol. Tissue processing, paraffin embedding, and sectioning (5 µm) of the colon was done following routine procedures (see section 2.3.1). Colon pathology was graded blind on H&E stained sections using an established

Chapter 3: The effects of azathioprine on bone health in an *in vivo* model of IBD

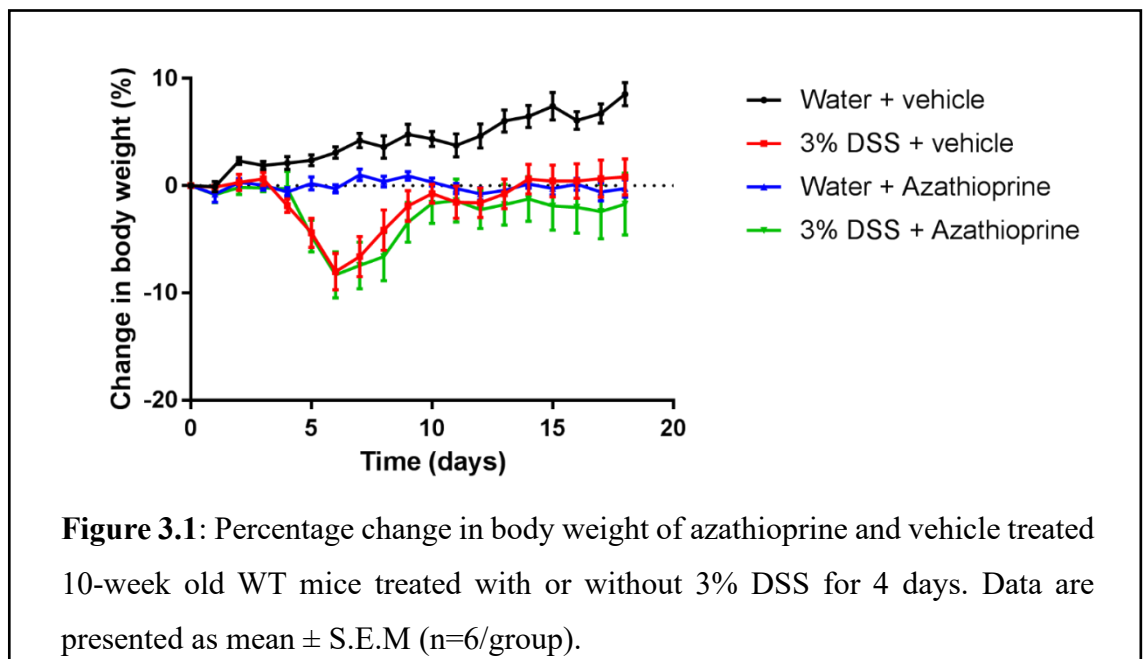
histological grading scheme by Prof. Elspeth Milne at the University of Edinburgh, following (see section 2.3.6).

3.2.3 Bone phenotyping

Following dissection, the right tibia bone from each mouse was scanned with an 1172 X-Ray microCT (Skyscan, Belgium) at 5 μm resolution. Changes in trabecular microarchitecture and cortical geometry were determined using established methods (see section 2.2). The left tibia from all mice was decalcified in 10% EDTA following fixation, and tissue processing, paraffin embedding, and sectioning (5 μm) conducted following routine procedures (see section 2.3.1). Histological staining was carried out as described in sections 2.3.2 – 2.3.5. ELISA analysis of bone formation (P1NP) and bone resorption (Ctx) were conducted on serum collected from all mice (see section 2.4).

3.3. Results

3.3.1 The effect of DSS treatment on body weight and longitudinal bone growth of mice

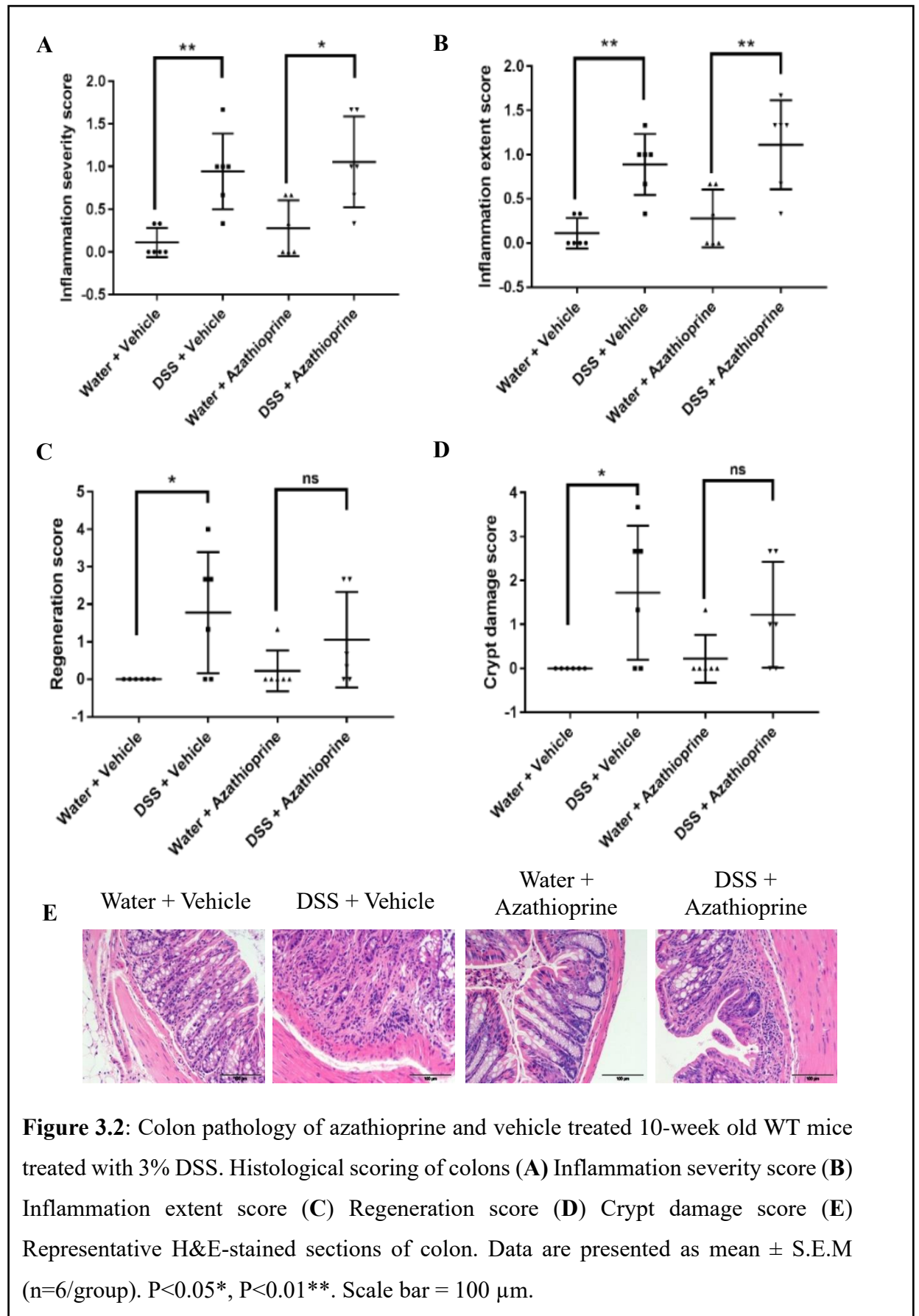


	Vehicle Treated		Azathioprine treated	
	Water	DSS treated	Water	DSS treated
Tibia (mm)	17.3 ± 0.1	17.4 ± 0.1	17.1 ± 0.2	17.4 ± 0.1

Table 3.1: Tibia length measurements of vehicle and azathioprine treated 10-week old WT mice at day 18 of DSS study. Data are presented as mean ± S.E.M (n=6/group). ^a significantly different from vehicle treated control mice (P<0.0003*).

To assess the effects of DSS-induced colitis, azathioprine and vehicle treated mice were given 3% DSS for 4 days. The dose and duration of the DSS treatment was based on previous studies using the same mouse strain (Dobie et al., 2018). During the DSS treatment period (0-4 days), no significant weight loss was observed in any mouse treatment groups (Fig. 3.1). Independent of azathioprine treatment, mice exhibited a rapid and significant weight loss from day 4 following DSS treatment (up to 7% in comparison to non-DSS (water) treated mice, P<0.0045). Following this period of weight loss, DSS/vehicle treated mice continued to gain weight to the end of the study, similar to the water/vehicle treated mice (Fig. 3.1). However, after an initial weight gain following the period of weight loss, DSS/azathioprine treated mice plateaued in their weight gain from day 10 onwards (Fig. 3.1). Similarly, water/azathioprine treated mice showed no significant weight gain throughout the experiment (Fig. 3.1). Full details of the weight measurements over the 18-day treatment period can be seen in Appendix Table 1. DSS treatment in vehicle and azathioprine treated mice had no effect on tibia length (Table 3.1).

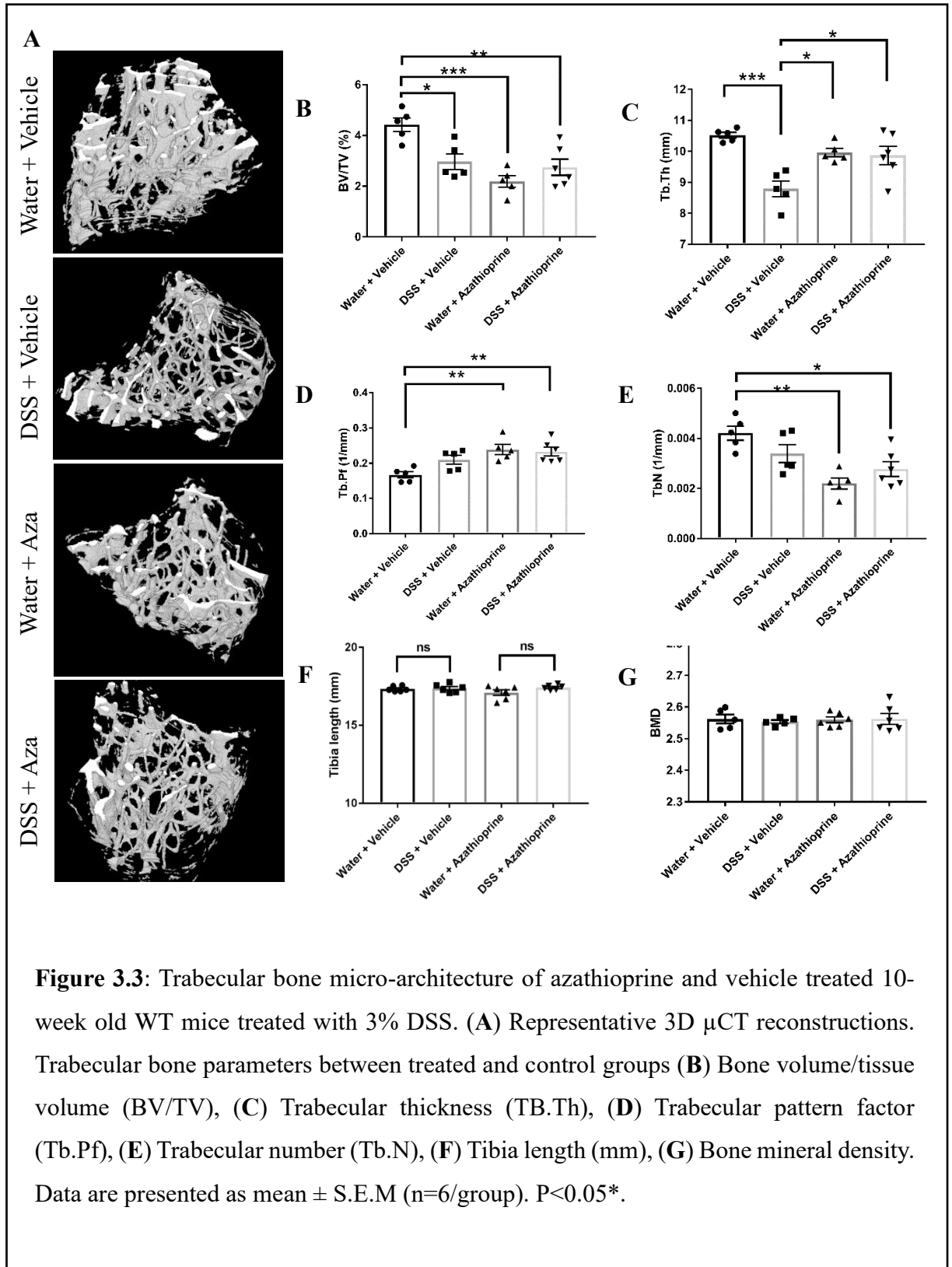
3.3.2. Colon pathology in DSS-treated mice



Chapter 3: The effects of azathioprine on bone health in an *in vivo* model of IBD

To assess the effects of DSS on mucosal integrity, detailed histological analysis was performed on the colon from water and DSS-treated vehicle and azathioprine-treated mice. Histological scores for all parameters were minimal in the non-DSS treated (water) mice, and there were no notable differences observed with azathioprine treatment in this group (Fig. 3.2). In contrast, histological analysis of the colon from DSS-treated mice revealed significant increases in inflammation severity (Fig. 3.2A, $P < 0.0076$) and extent (Fig. 2B, $P < 0.0059$) scores in comparison to water treated mice, consistent with previous studies and indicative of colitis induction. It was also observed that treatment with azathioprine in the DSS model provides partial protection to the colon through increased tissue regeneration (Fig. 3.2C) and no significant effect on the crypt damage score (Fig. 3.2D), in contrast to the vehicle treated mice ($P < 0.0077$).

3.3.3. Bone phenotype of DSS treated mice

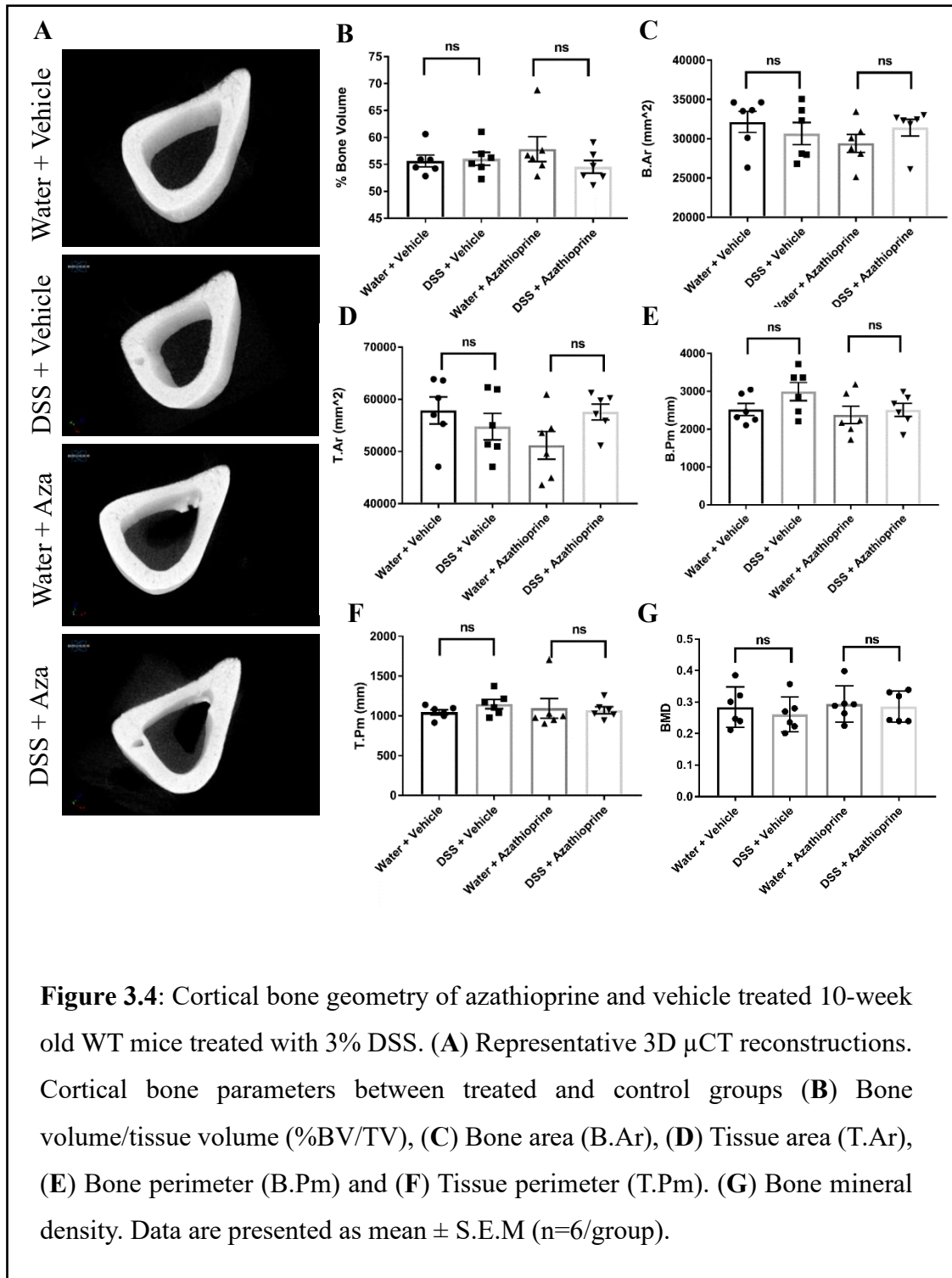


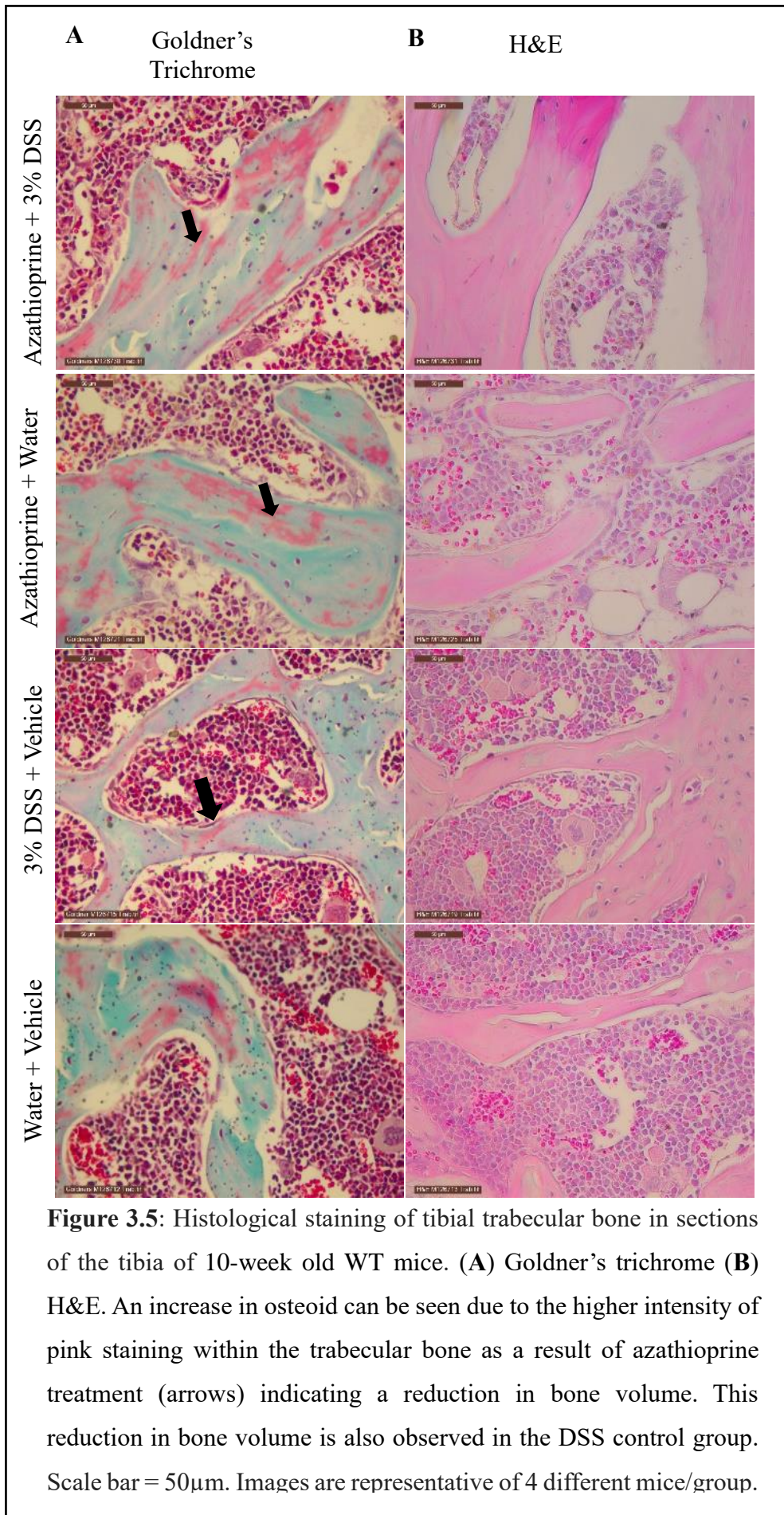
Chapter 3: The effects of azathioprine on bone health in an *in vivo* model of IBD

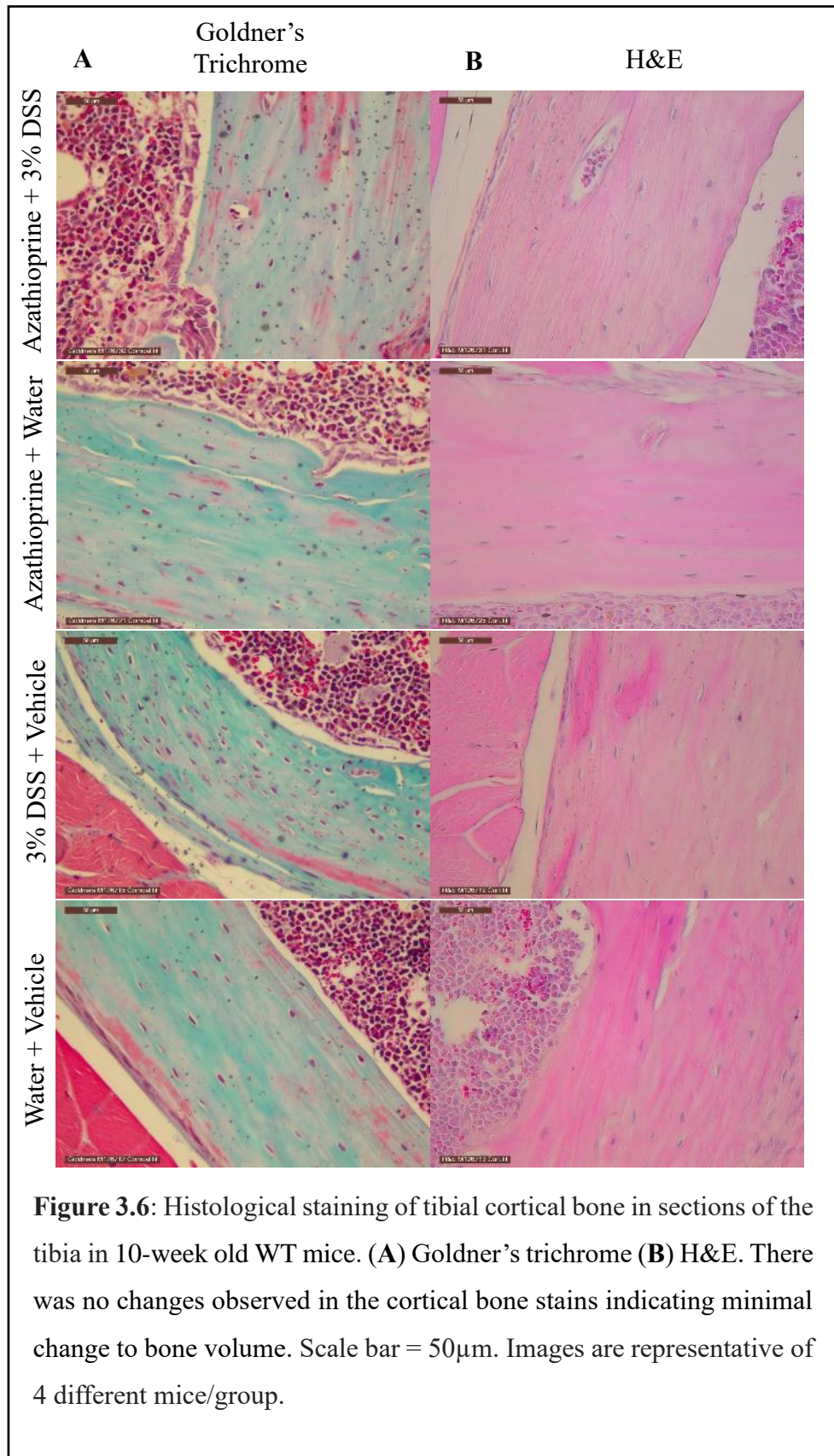
DSS-induced colitis has previously been shown to have detrimental effects on bone quality (Dobie et al., 2016; Hamdani et al., 2008; Harris et al., 2009). In accordance with these studies, DSS/vehicle treated mice showed worsened trabecular microarchitecture compared to water/vehicle treated mice as demonstrated by μ CT (Fig. 3.3). Thus, confirming DSS induced the expected colitis-mediated effects on bone health. Specifically, DSS/vehicle treated mice exhibited a significant decrease in trabecular thickness (Fig. 3.3C, $P < 0.0003$) compared to the water group, with further decreases in BV/TV (Fig. 3.3B, $P < 0.0141$), and, although not significant, trabecular number (Fig. 3.3E) also observed. Treatment with azathioprine appeared to provide partial protection against the DSS-induced bone loss as trabecular thickness was significantly increased in comparison to the vehicle treated DSS mice (Fig. 3.3C, $P < 0.0136$). However, this protection was not observed in any of the other parameters.

Most interestingly, azathioprine treatment alone had a significant detrimental effect on the bone health of mice, independent of DSS treatment. Indeed, significant decreases were observed in BV/TV (Fig. 3.3B, $P < 0.0003$), and trabecular number (Fig. 3.3E, $P < 0.0011$), with a concurrent significant increase in trabecular pattern factor (Fig. 3.3D, $P < 0.0042$) indicative of a more disorganised trabecular structure.

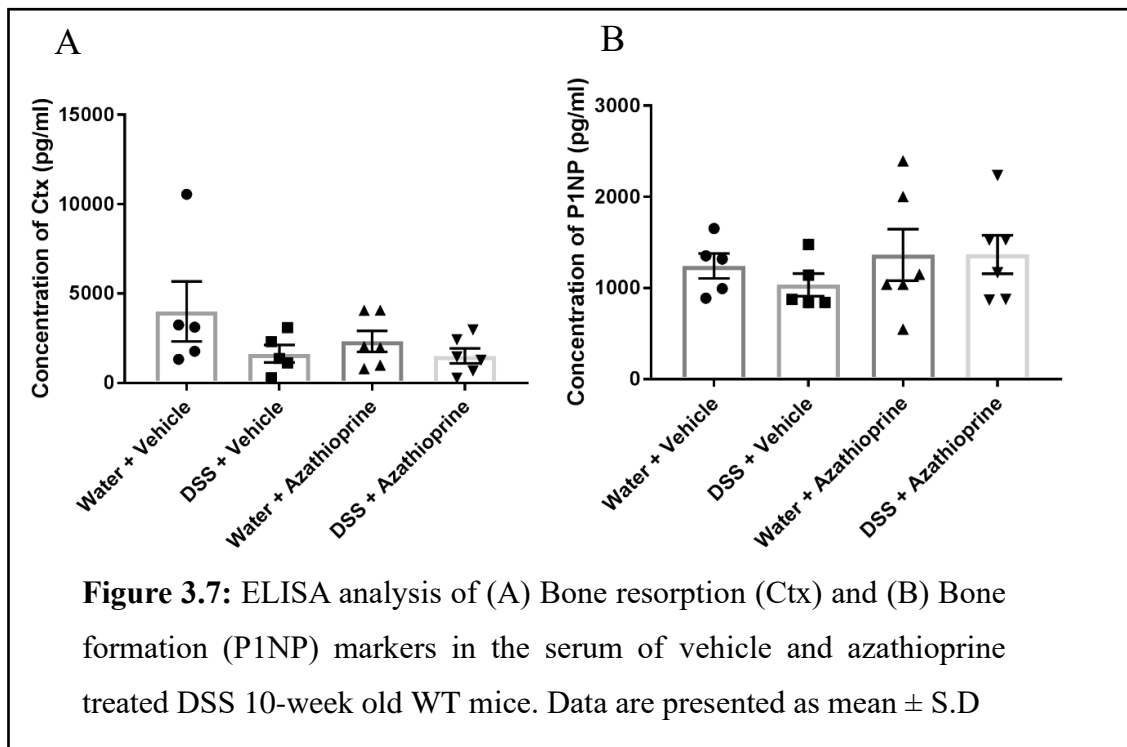
The cortical bone was examined by μ CT however there was no significant differences observed in any parameters between the treatment groups (Fig. 3.4). Histological analysis of the tibia sections confirmed the results seen from the μ CT analysis with a reduction in bone volume (indicated by increased red osteoid staining) in the trabecular bone in both the DSS treated mice and those treated with azathioprine (Fig. 3.5A). Similarly, little differences were observed in the cortical bone (Fig. 3.6A).







3.3.4. ELISA



ELISA assays were carried out to test for the bone formation and resorption markers, P1NP and Ctx respectively.

Unfortunately, there was found to be no significant changes between treatment groups in the serum concentration of Ctx (bone resorption) (Fig. 3.9A) or P1NP (bone formation) (Figure 3.9.B)

3.4. Discussion

It is thought that increased inflammation leads to bone loss in IBD patients due to malabsorption of nutrients such as vitamin D and calcium (Bianchi, 2010). However, other direct mechanisms may exist and the development of targeted therapies for this bone loss requires a better understanding of the underlying cellular mechanisms. Therefore, in this chapter, I aimed to examine the effects of the commonly prescribed IBD drug azathioprine on bone health in an *in vivo* model of IBD, due to the known effects of azathioprine on autophagy.

Osteoporosis is a metabolic disease of the bone which is characterised by a reduction in bone mineral density and alterations in bone structure (Bianchi, 2010). It is seen as a secondary symptom of IBD and patients who suffer from IBD often experience bone loss and are 40% more likely to suffer from fractures compared to healthy individuals (Ali et al., 2010). DSS-induced colitis has previously been shown to have detrimental effects on bone quality (Dobie et al., 2018; Hamdani et al., 2008; Harris et al., 2009). In accordance with these studies, the model used here showed the expected worsened bone trabecular microarchitecture with DSS treatment in mice.

Here it was found that azathioprine provided partial protection against bone loss in IBD as there was significantly increased trabecular thickness in comparison to vehicle treated mice, although this was not observed in any of the other parameters. However, when azathioprine was administered alone it was found to be detrimental to bone microarchitecture in comparison to the vehicle control, as indicated by the significant reductions in both the overall bone volume, the number of the trabeculae as well as increased trabecular disorganisation (trabecular pattern factor).

The treatment with thiopurines such azathioprine and 6-mercaptopurine has previously been found to be negatively associated with height in children with crohn's disease. It

Chapter 3: The effects of azathioprine on bone health in an *in vivo* model of IBD

was observed that thiopurines were linked to a reduction in lean tissue mass, weight and BMI scores in pediatric CD patients (Gupta et al., 2018). This compliments the findings in this study where it was observed that the tibia length of mice treated with azathioprine was reduced indicating that the use of thiopurine treatment may result in reduced growth in patients.

Azathioprine has previously been linked to an increase in fracture risk in humans. However fracture risk was not increased in common osteoporotic sites such as the hip or spine, but rather an increase in the overall skeletal fracture risk was observed (Vestergaard et al., 2006). In addition, it has been suggested that azathioprine can disrupt the bone remodelling process by suppressing T lymphocytes causing disturbances in the RANKL system responsible for osteoclast differentiation (Cegiela et al., 2013). Cegiela et al., found that although the length and diameter of the bones remained unchanged, azathioprine caused an overall reduction in femur and tibia mass in a rat model, whilst also reducing the calcium content. Further, the thickness of the trabeculae in the femur was found to be reduced in rats when treated with azathioprine in both the distal epiphysis and metaphysis (Cegiela et al., 2013). These findings complement my findings that the administration of azathioprine may contribute to overall bone loss and trabecular bone deterioration. This suggests that azathioprine alone may therefore not be a suitable drug of choice in IBD patients who are more at risk of osteoporotic bone fractures, such as the elderly.

Histopathological analysis of the colon revealed successful induction of colitis in DSS treated mice, however also revealed no differences in the severity or extent of inflammation in azathioprine treated mice, in comparison to vehicle-treated mice. This therefore suggested that the effects of azathioprine are direct on the skeleton in IBD. It has previously been found that azathioprine induces autophagy in peripheral blood mononuclear cells and colorectal cancer cells (Hooper et al, 2019; Chaabane & Appell,

Chapter 3: The effects of azathioprine on bone health in an *in vivo* model of IBD

2016). In addition, autophagy has previously been found to play a protective role in bone health and when autophagy becomes dysregulated it can have a harmful effect on bone (Pierrefite-Carle et al., 2015). However, the effect of azathioprine on autophagy in bone has yet to be determined.

In conclusion, the data detailed in this chapter show that although azathioprine may provide partial protection against bone loss in IBD, it was found to cause detrimental effects when administered to a healthy control group. Because of this the mechanism of action of azathioprine needs to be better understood, to allow for better quality of treatment for IBD patients.

Chapter 4

The effects of azathioprine on autophagy in bone

4.1. Introduction

The administration of azathioprine to the murine DSS model detailed in chapter 3 revealed detrimental effects on the skeleton in both the healthy mice and those with colitis. Due to the lack of changes in the severity or extent of colon inflammation with azathioprine treatment, this may suggest that the detrimental effects on the skeleton may occur as a direct result of treatment. It has been previously shown that azathioprine induces autophagy in peripheral blood mononuclear cells and colorectal cancer cells (Hooper et al, 2019; Chaabane & Appell, 2016). Therefore, we hypothesised that autophagy may be induced in the skeleton as a survival mechanism to compensate the adverse effects caused by azathioprine treatment.

Autophagy involves the removal of damaged organelles or proteins from the cell (Shen et al., 2018). The process begins with the formation of a phagophore which engulfs the cargo destined for degradation, thereby forming the autophagosome. The autophagosome then binds with a lysosome in the cell cytoplasm where the contents are degraded via lysosomal hydrolases. The degradation products are then released back into the cytoplasm and recycled (Aburto et al., 2012).

A complex is formed on the phagophore which includes LC3, the mammalian homologue of Atg8, which is found on both the outer and inner membranes of the autophagosome. There are two forms of LC3 - LC3I and LC3II. During the induction of autophagy, LC3-I is converted to LC3II by the cleaving of LC3I by Atg4 to allow for the conjunction to phospholipids. This is essential for the formation of the autophagosomes (Iii et al., 2010, Glick et al., 2010) and LC3 is therefore a dependable way to monitor autophagy activity as the amount of LC3-II correlates with the number of autophagosomes. p62 is an adaptor protein that is degraded by autophagy due to its binding with LC3 (Lilienbaum, 2013).

Chapter 4: The effects of azathioprine on autophagy in bone

Therefore, when autophagy is disrupted, levels of p62 increase and therefore p62 can be a good marker of autophagy activation (Duran et al., 2016).

A number of studies have found that the activation of autophagy is beneficial for bone health. It has previously been shown that autophagy is increased during osteoblast differentiation and ECM mineralisation, and that the inhibition of autophagy reduces ECM mineralisation (Pierrefite-Carle et al., 2015). Further, there are a number of studies suggesting that autophagy induction may protect against bone loss in osteoporosis (Zahm et al., 2011). However, the role of autophagy in IBD-related osteoporosis has yet to be established.

Therefore, in this chapter, I aimed to establish the effects of azathioprine on autophagy in the skeleton in the (DSS) model of IBD in mice, and to characterise the effects of azathioprine on an *in vitro* osteoblast cell culture model.

4.2. Materials and methods

4.2.1. Tissue processing and immunohistochemistry

Following tissue dissection and fixation (section 2.3.1), the left tibia from all mice was decalcified in 10% EDTA. Tissue processing, paraffin embedding, and sectioning (5 μ m) of the tibia was done following routine procedures. Immunohistochemical labelling for LC3 and p62 (see Table 2.2 & 2.3) was carried out using a Vectastain ABC kit, according to the manufacturer's instructions (section 2.3.2). The immunohistochemical expression was quantified using ImageJ software.

4.2.2. Cell culture and treatment

Murine MC3T3 osteoblast-like cells were cultured in α MEM supplemented with 10% FBS and 5% penicillin/streptomycin. Cells were plated into 6 well plates at 1×10^5 cells

Chapter 4: The effects of azathioprine on autophagy in bone

per well (section 2.5) until confluency at which point they were cultured for up to 10 days with the addition of 50 µg/ml ascorbic acid and 5 mM βGP (section 2.6). The cells were then treated for 24 hours with 120 µM azathioprine or 10 µM rapamycin as the positive control. Additionally, 80 nM bafilomycin was also included with the positive control and the azathioprine test group. Bafilomycin induces autophagosome accumulation by blocking the fusion of autophagosomes and lysosomes helping to measure autophagy as it results in an accumulation of LC3. The cells were left to incubate for 24 hours before being scrapped for RNA and protein.

4.2.3. RNA analysis of MC3T3 cells

RNA was isolated from MC3T3 cells using a Qiagen RNeasy kit (section 2.7.1) and reverse transcribed to cDNA (section 2.7.2). For qPCR analysis, cDNA was diluted to 5 ng/µl using RNase free water and analysed using a StepOne Real-Time PCR system. The cycle threshold (Ct) values obtained were normalised to *Atp5b* in MC3T3 cell lines and the expression of osteoblast genes (Table 2.1) were calculated using the $2^{-\Delta\Delta C_t}$ method (Livak & Schmittgen, 2001).

4.2.4. Protein extraction and western blot

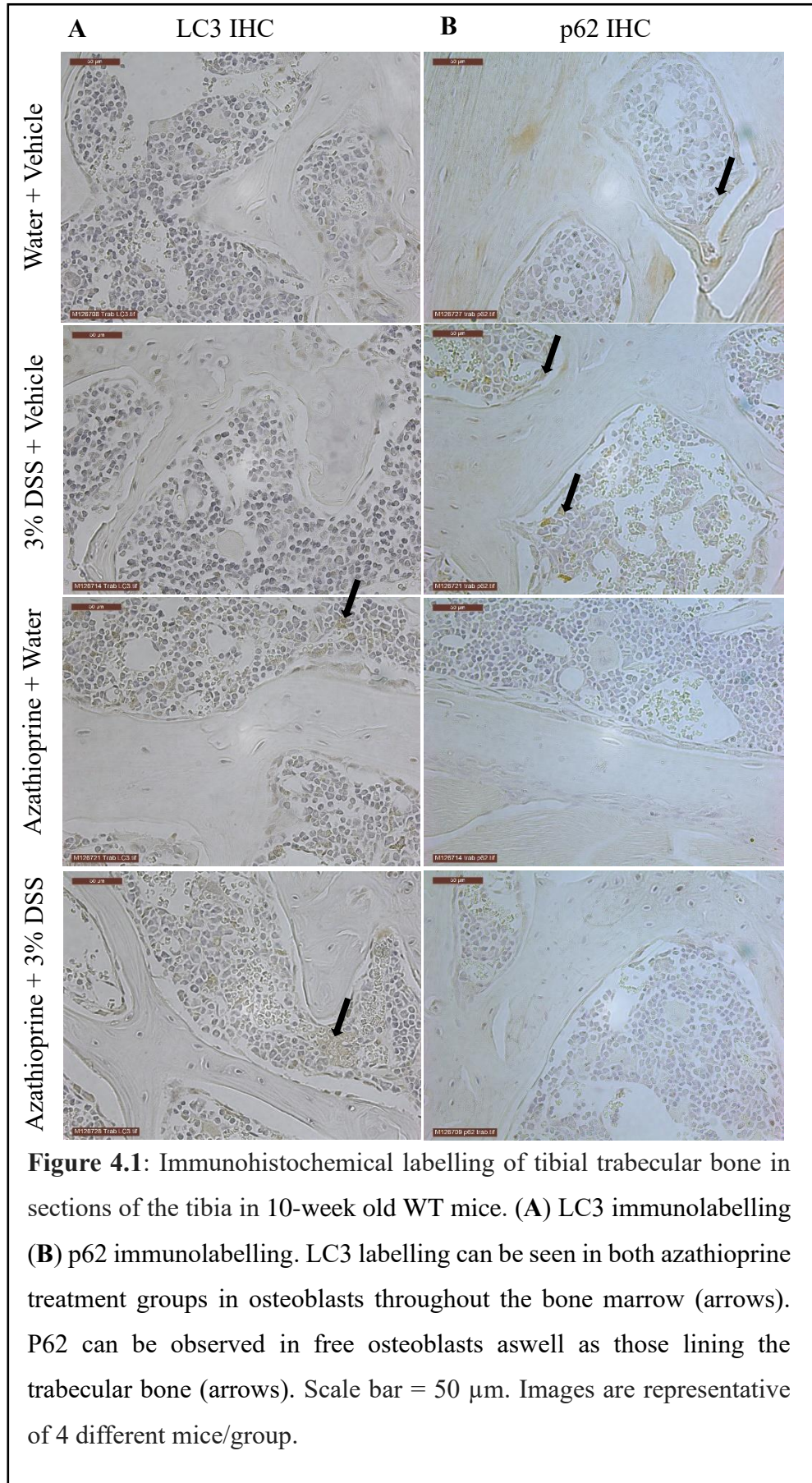
Proteins were extracted from MC3T3 cells at 24 hours in RIPA buffer as described in section 2.8.1. Protein samples were quantified using a DC assay (section 2.8.2) and prepared for western blot analysis. Proteins were loaded on a 4-12% Bis Tris protein gel and then transferred to PVDF membrane. The membrane was blocked using Odyssey buffer before being probed for the autophagy markers LC3 and p62 (Tables 2.2 & 2.3). Following exposure to an appropriate secondary antibody, proteins were detected using the Licor system. Protein loading was confirmed by re-probing the membrane with actin antibody (1:1000).

4.3. Results

4.3.1. Autophagy induction in azathioprine treated mice

To examine whether azathioprine affects autophagy *in vivo*, immunohistochemistry for the autophagy markers LC3 and p62 were conducted.

Increased LC3 labelling was observed in azathioprine treated bones vs vehicle treated (Fig. 4.1A, Fig. 4.3A & B), independent of DSS treatment. Specifically, LC3 was found in the osteoblasts lining the trabecular bone, in the osteocytes, and throughout the bone marrow. Increased LC3 labelling was also observed in the osteoblasts lining the cortical bone compared to those treated with the vehicle (arrows, Fig. 4.2A, Fig. 4.3A). The DSS treatment alone was not successful in inducing autophagy however the treatment with azathioprine in the DSS group produced increased LC3 labelling in both trabecular and cortical bone (Fig. 4.1A, 4.2A & 4.3A & B). p62 levels were low in almost all treatment groups apart from an increase in the cortical bone in the two vehicle control groups (Fig. 4.1B & 4.2B, 4.3C & D). Together, this indicates that autophagy is induced by azathioprine *in vivo*, independent of DSS treatment. IgG labelling was utilised as a control in all IHC experiments (Appendix 2).



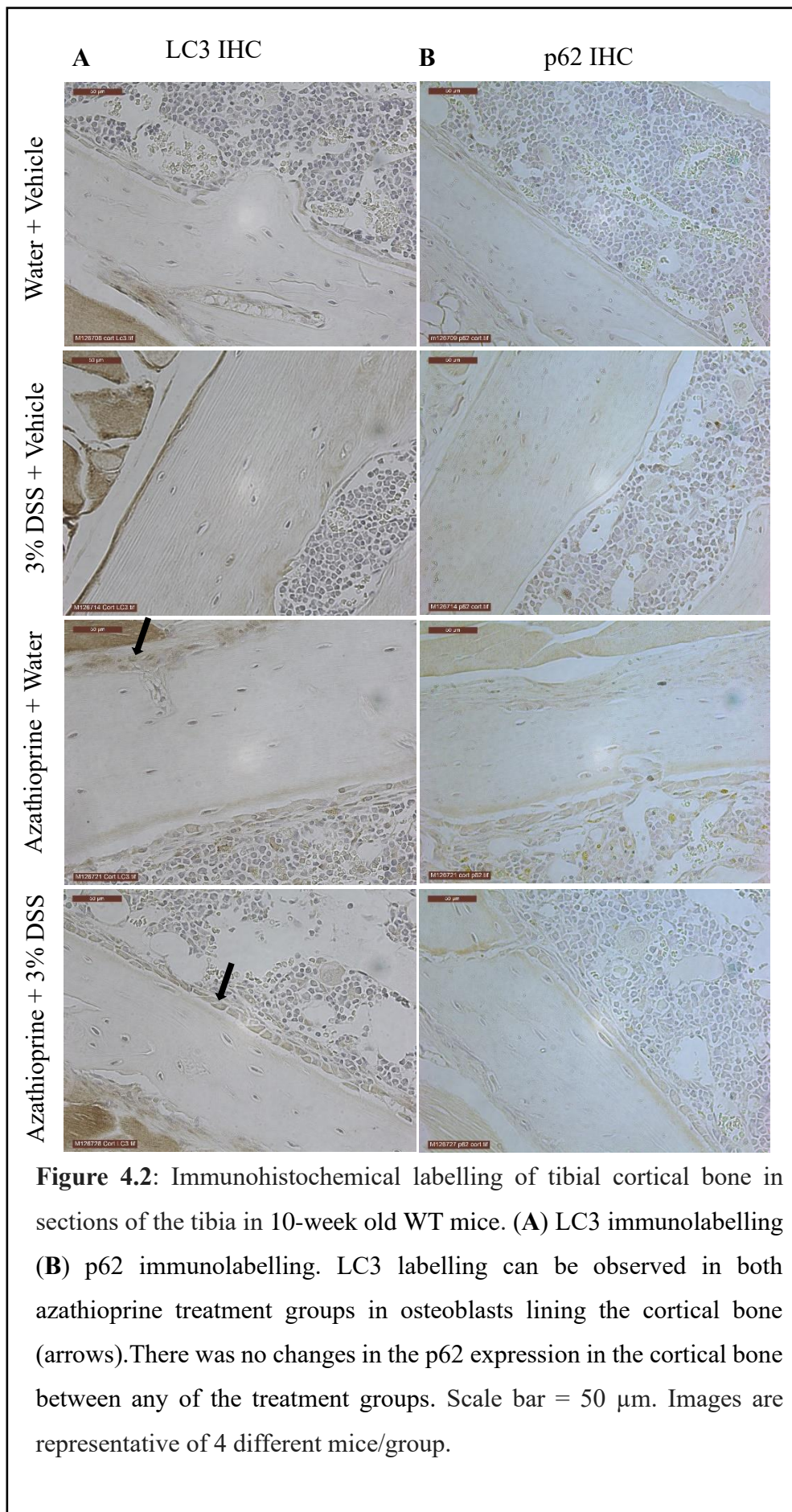


Figure 4.2: Immunohistochemical labelling of tibial cortical bone in sections of the tibia in 10-week old WT mice. (A) LC3 immunolabelling (B) p62 immunolabelling. LC3 labelling can be observed in both azathioprine treatment groups in osteoblasts lining the cortical bone (arrows). There was no changes in the p62 expression in the cortical bone between any of the treatment groups. Scale bar = 50 μm. Images are representative of 4 different mice/group.

Chapter 4: The effects of azathioprine on autophagy in bone

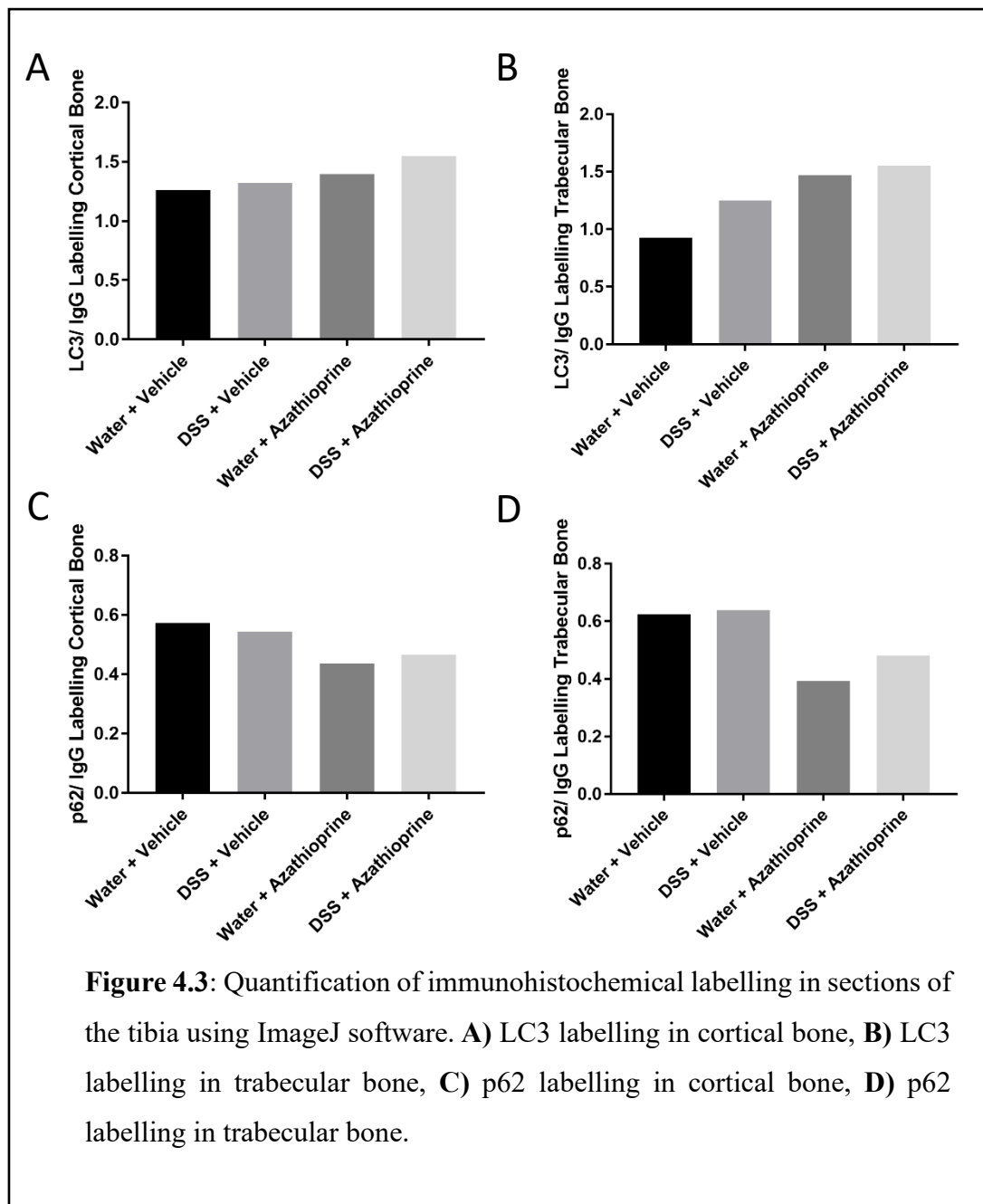


Figure 4.3: Quantification of immunohistochemical labelling in sections of the tibia using ImageJ software. **A)** LC3 labelling in cortical bone, **B)** LC3 labelling in trabecular bone, **C)** p62 labelling in cortical bone, **D)** p62 labelling in trabecular bone.

4.3.2. Effect of azathioprine treatment on osteoblasts

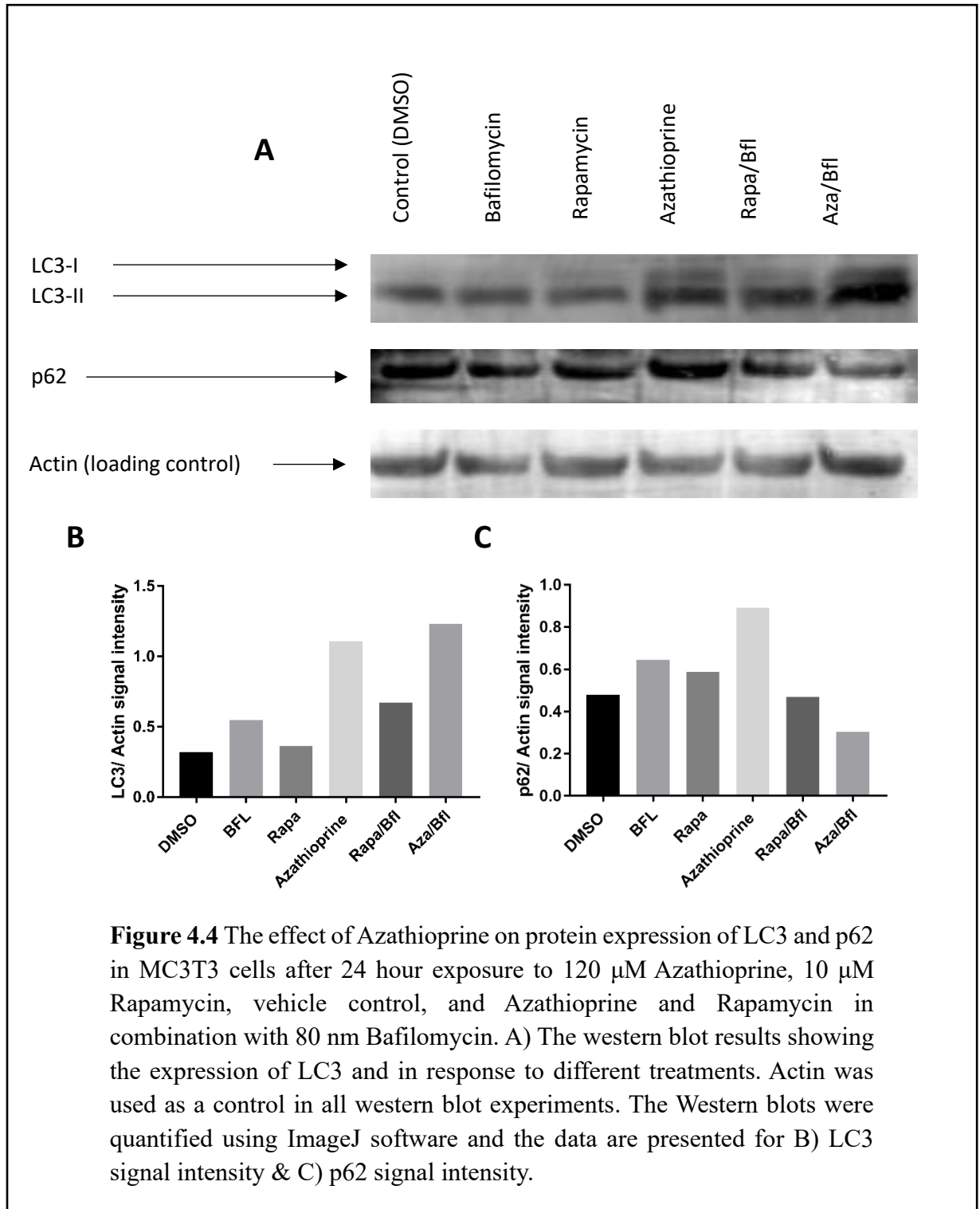
Azathioprine was found to have detrimental effects on bone health in the *in vivo* model whilst also inducing autophagy in the skeleton of both the healthy group and the group with DSS-induced colitis. We therefore next attempted to examine the effects of azathioprine on bone markers and autophagy induction in an osteoblast cell line. MC3T3 cells were treated with 120 μM azathioprine or 10 μM rapamycin (positive control for

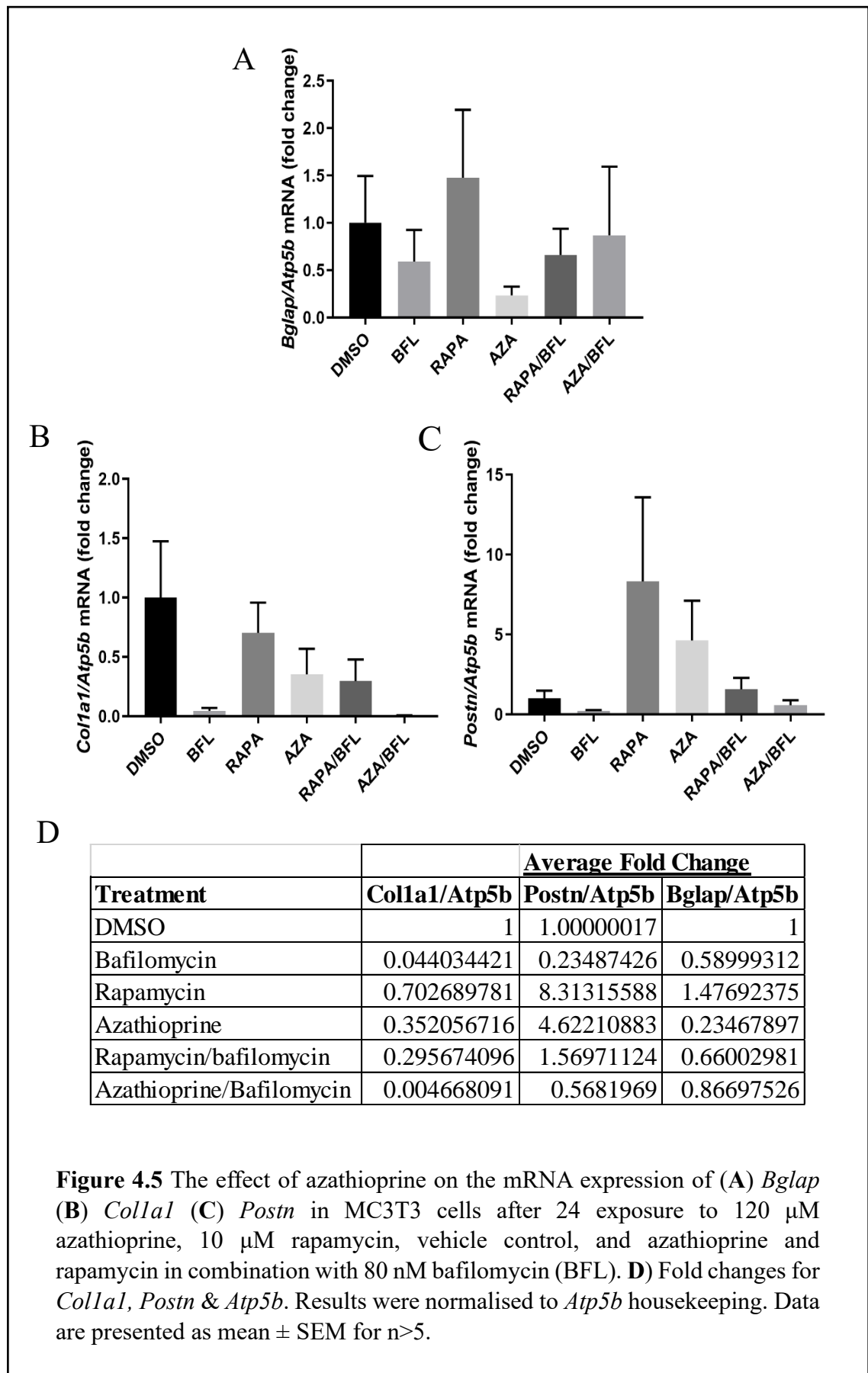
Chapter 4: The effects of azathioprine on autophagy in bone

autophagy induction). Bafilomycin was also used in combination with both treatments as it results in the augmentation of LC3-II by blocking the fusion of the autophagosome to the lysosome (Yamamoto et al., 1998).

A modest increase in autophagy was observed in the MC3T3 cells treated with azathioprine and rapamycin in combination with bafilomycin, as indicated by the increased LC3-II expression in comparison to the control observed by western blot (Fig. 4.4A & B). This was also detected with treatment of azathioprine alone, however, this was not observed in the cells treated with rapamycin (Fig. 4.4A & B). There were little changes in LC3-I expression between treatment groups (Fig. 4.4A). The observed reduction in p62 protein expression also suggests that autophagy was induced in MC3T3 cells treated with azathioprine and rapamycin in combination with bafilomycin (Fig. 4.4A & C).

There were no significant changes seen in the mRNA expression of the bone turnover markers osteocalcin (*Bglap*), collagen type I (*Coll1a1*) and periostin (*Postn*) in azathioprine or rapamycin treated MC3T3 cells in comparison to control cultures by RT-qPCR (Fig. 4.5). Although no significant changes were observed there was a large increase in periostin expression in both groups treated with azathioprine and rapamycin alone (Fig. 4.5C). This may indicate that the modest effects on autophagy observed with this treatment regime may result in protection against bone damage caused by IBD due to the ability of periostin to increase the adhesion capacity of osteoblast cells to matrix proteins.





4.4. Discussion

We hypothesised that autophagy may be induced in the skeleton as a survival mechanism to compensate the adverse effects caused by azathioprine treatment. Azathioprine has already been shown to induce this process in peripheral blood mononuclear cells and colorectal cancer 9kcells (Hooper et al, 2019; Chaabane & Appell, 2016).

Autophagy maintains homeostasis through protein degradation and the use of destroyed cell organelles for new cellular formation (Hocking et al., 2012). Upon the induction of autophagy, LC3-I becomes lipidated and becomes LC3-II (Nollet et al., 2014) and because of this, the detection of LC3 is a reliable marker of autophagy detection. In this study it can be clearly seen that autophagy has been induced in the skeleton by azathioprine in both the group with DSS induced colitis and the healthy group. Therefore, we have demonstrated, for the first time, that azathioprine is an effective inducer of autophagy in the bone. This was confirmed by p62 labelling which was reduced in both groups that received azathioprine treatment. p62 is thought to act as a cargo receptor during autophagy and is degraded during the binding to LC3 which allows the cargo to be enclosed by autophagosomes (Lamark et al., 2009; Itakura & Mizushima, 2011).

Together, these data indicate that azathioprine can induce autophagy in the skeleton of both healthy mice and those with DSS induced colitis. The reasons for this are currently speculative as it is currently not known whether autophagy is indirectly induced as a survival mechanism to cope with the adverse effects caused by azathioprine on bone health. Similarly, because azathioprine does not protect against IBD-induced bone deterioration as effectively as predicted, the mechanism of azathioprine action needs to be better understood before a better level of care for patients can be provided.

The main function of osteoblasts is to synthesize and mineralise the osteoid for bone formation (Brandi, 2009). There are many known markers of the osteoblast phenotype

Chapter 4: The effects of azathioprine on autophagy in bone

including osteocalcin (*Bglap*), periostin (*Postn*) and collagen type 1 (*Colla1*) (Flores-Silva et al., 2015, Garnero, 2009). Osteocalcin is a non-collagenous, vitamin K-dependant protein that is produced by osteoblasts and an abundance promotes the deposition of mineral substance (HA) (Razzaque, 2011). Periostin is an extracellular matrix protein highly expressed in collagen-rich tissues and is involved in tissue remodelling and its altered function is associated to numerous pathological processes (Cobo et al., 2016). Collagen type 1 is secreted by osteoblasts and acts as the scaffold for the deposition of hydroxyapatite crystals in bone mineralisation (Van Dijk et al., 2010; Nudelman et al., 2010).

The effects of azathioprine on osteoblast function are currently unknown, however, the effects of rapamycin are well documented, albeit somewhat controversial in their findings. It has been shown that rapamycin, in the presence of lipopolysaccharides, can promote the differentiation of human embryonic stem cells (hESCs) into mature osteoblasts by modulating mTOR signalling (Lee et al., 2010; Li et al., 2017). However, it was also found that rapamycin inhibits osteoblast proliferation and differentiation in MC3T3-E1 cells. It was observed that even at low concentrations (0.1-20 nM), rapamycin reduced osteocalcin and osterix mRNA expression in differentiating MC3T3-E1 osteoblasts, as well as reducing their mineralisation capacity (Singha et al., 2008). Rapamycin however had no effect on these parameters in fully differentiated osteoblasts (Singha et al., 2008).

In this study, neither azathioprine or rapamycin had any effect on the bone phenotype in the osteoblast MC3T3 cell line and a minimal effect on autophagy in these cells. This could be due to a number of reasons. *In vitro* systems are an isolated cell type whereas an *in vivo* model has lots of different cell types involved and a number of complimentary mechanisms and pathways. In addition, a cell line can often show altered morphology and can often differ genetically from their tissue origin. In contrast, primary cell lines are

Chapter 4: The effects of azathioprine on autophagy in bone

isolated directly from tissues and retain the normal morphology maintain the same markers and functions that would be observed in an *in vivo* model. Therefore, the drug treatment may respond differently when applied to a primary cell culture as it is more like to mimic the results of the *in vivo* study.

In conclusion, the results of this chapter have indicated that azathioprine induces autophagy in bone in both healthy and DSS-treated mice. However, there was only a small increase in autophagy marker expression in our *in vitro* model and only when azathioprine was given in combination with bafilomycin. This modest autophagy induction had no effect on the mRNA expression of known osteoblast makers. Further work is required to determine the exact role that autophagy plays in bone remodelling with azathioprine treatment.

Chapter 5

Final discussion

5.1. General discussion

Autophagy plays a vital role in several different pathways within the body including bone remodelling, and in various diseases such as IBD (Valenti et al., 2016; (Henderson & Stevens, 2012). Bone remodelling involves both bone-forming osteoblasts and bone-resorbing osteoclasts and any imbalance in this process can result in osteoporosis. Osteoporosis is characterised by low bone mass and can result in higher fracture risk (Sambrook & Cooper, 2010). It is often seen as a secondary disease in patients with IBD, with the prevalence of osteoporosis being reported in a range of 12-42% (Ali et al., 2010; Miznerova et al., 2013).

Because of the risk of developing osteoporosis, especially in susceptible patients, the mechanism of action of IBD drugs needs to be better understood to allow for more targeted therapy for IBD patients. Thiopurines are widely used in the treatment of IBD and have been proven to be highly effective, however up to a third of patients have to stop treatment with thiopurines due to adverse side effects (Dart & Irving, 2017; Warner et al., 2018). Therefore, understanding the mechanism of action of the drugs is of increasing importance so that thiopurine therapy can be tailored and personalised to the individual receiving treatment (Dart & Irving, 2017).

In this thesis, I looked at the effect of azathioprine, a commonly prescribed immune-suppressive IBD drug, on the skeleton in a DSS-induced colitis *in vivo* model. Moreover, to enable examination of the mechanism of azathioprine action, preliminary experiments were conducted on an osteoblast cell line.

The DSS-model of IBD is most often used to look at histological changes in the colon associated with chronic IBD. The colitis induced in the DSS-model happens as a result of the deterioration of the epithelial barrier which causes an increase in cell apoptosis and a reduction in proliferation (Hamdani et al., 2008). DSS-induced colitis has also been

Chapter 5: Final discussion

shown to cause reduced bone health in young male mice, both juvenile mice at 4 weeks old and young adults at 10 weeks. Trabecular and cortical bone compartments were found to be affected in younger mice whilst altered microarchitecture was observed in older mice (Hamdani et al., 2008; Harris et al., 2009; Dobie et al., 2018).

Azathioprine treatment in my *in vivo* model detailed here resulted in trabecular bone loss, independent of colitis induction. Trabecular bone is less dense than cortical bone which makes it weaker and more flexible. Trabecular bone also has a higher level of porosity in comparison to cortical bone. The increase porosity allows more free surfaces which results in trabecular bone exhibiting more metabolic activity in comparison to cortical bone which causes it to be more responsive to different stimuli (Jacobs., 2000). Because of this trabecular bone is more susceptible to changes such as altered microarchitecture than cortical bone which could explain the lack of changes in cortical bone geometry following treatment with azathioprine seen here. Our results confirm what has been previously found in a study on a rat model where bone loss was also observed following treatment with azathioprine (Cegiela et al., 2013). Although the length of the bones was not reduced, the trabeculae was found to be thinner in both studies and an overall loss of bone mass was observed (Cegiela et al., 2013). This suggests that azathioprine alone may therefore not be a suitable drug of choice in IBD patients who are more at risk of osteoporotic bone fractures, such as the elderly. However, there are very few studies looking at the effect of azathioprine on bone health and further work is required to elucidate these effects (see section 5.2).

In this thesis, we also assessed the effects of DSS on the mucosal integrity in our mouse model. Acute and chronic colitis is characterised by different changes to the colon. Acute inflammation is linked with epithelial degradation and an increase in neutrophils. Chronic inflammation however is associated with an increase in mononuclear leukocytes and crypt regeneration (Dobie et al., 2018). The histological analysis in this study confirms

Chapter 5: Final discussion

that the current design used herein is sufficient to induce chronic inflammation in the *in vivo* model. In the DSS treated mice significant crypt damage was observed along with an increase in inflammation severity. The azathioprine treatment was seen to provide partial protection against DSS induced crypt damage, however there were no significant changes seen in any of the parameters between the vehicle and azathioprine DSS treatment groups. Chronic inflammation has previously been linked with autophagy, and it has been observed that autophagy influence the development of inflammatory cells, including lymphocytes, neutrophils and macrophages, all of which play crucial roles in the development of inflammation (Qian et al., 2017).

Furthermore, azathioprine has previously been shown to induce autophagy in peripheral blood mononuclear cells and colorectal cancer cells (Hooper et al, 2019; Chaabane & Appell, 2016). Autophagy has previously been implicated in skeletal maintenance, increased autophagy has been found during osteoblast differentiation and mineralisation and it was observed that autophagy is highly expressed in osteocytes in response to starvation and hypoxia (Pierrefite-Carle et al., 2015). In this study, we found that azathioprine induced autophagy in the bone in the mouse model in both the healthy control group and the mice treated with DSS. However, this was not observed in our preliminary experiments looking at autophagy markers following azathioprine treatment in MC3T3 osteoblast cells. This could be due to the inability of azathioprine to induce autophagy in this osteoblast cell line or could be the concentration of azathioprine used in the study. There is very little research looking at the effect of azathioprine on bone and to our knowledge, no studies have been done to establish the effects of azathioprine on osteoblasts. Therefore, the drug concentration used in this study could be optimised in future work. Because of this, it is currently unclear as to whether the *in vivo* increase in autophagy seen in this study occurs as a direct effect of azathioprine or acts as a survival mechanism in response to adverse effects caused by the azathioprine treatment.

Chapter 5: Final discussion

Azathioprine can cause pancreatitis, hepatitis and fevers and in this thesis, it has been observed that treatment with azathioprine can cause a reduction in bone health. Therefore, it is important to determine whether autophagy is being induced in response to the cellular stress caused by these effects. This could be done by measuring apoptosis using microscopy and flow cytometry.

In conclusion, this thesis has identified that azathioprine provides partial protection against bone loss in DSS-treated mice, however when administered to a healthy group it causes significant bone loss. It has also been shown that azathioprine induces autophagy in the skeleton of healthy and colitis-induced mice. Preliminary results in the MC3T3 osteoblast cell line showed little change in osteoblast or autophagy maker expression, therefore highlighting the need for further work to identify the exact mechanism of action of azathioprine in bone.

5.2. Future work

The results presented in this study have shown that azathioprine can have detrimental effects to bone health *in vivo* and have confirmed that azathioprine can induce autophagy in the skeleton. However, further work is needed to identify the exact mechanism underpinning this.

To further examine the levels of inflammation in the *in vivo* model, blood tests may be carried out to test for proteins such as C-reactive protein (CRP) which increases in the presence of inflammation. CRP is a protein produced in hepatocytes in low quantities. During inflammation CRP expression increases due to the influence of IL-6, IL-1b and TNF (Tsampalieros et al., 2011).

To determine whether azathioprine is having a direct effect on bone via an autophagy-dependent mechanism, Atg5 deficient mice (Kuma et al., 2017) could be utilised to assess

Chapter 5: Final discussion

the effect of azathioprine on bone without the presence of autophagy. It has been previously observed in *Atg7* deficient mice that the suppression of autophagy in osteocytes mimics skeletal aging resulting in decreased trabecular and cortical bone volume and an increase in cortical porosity (Onal et al., 2013). Furthermore, it was found that autophagy deficient osteoblasts exhibit an increase in oxidative stress and produce NF- κ B. In vivo, it was observed that in osteoblast specific autophagy mice there was a decrease in trabecular mass (Nollet et al., 2014). This would allow the role of autophagy induced by azathioprine treatment to be confirmed by comparing the bone damage caused in autophagy deficient mice

In addition to examining azathioprine on an osteoblast cell line, primary cell lines could instead be utilised. Primary cell lines are isolated directly from the tissue and are able to preserve their original functions and characteristics. Immortalised cells, however, may lack the functions of normal cells that have been lost during their lifespan. Because of this, primary cells may therefore provide a more reliable examination of azathioprine effects on osteoblast function.

Investigating the effect of azathioprine on osteoclast function would be greatly beneficial in furthering our understanding of the cause of bone loss. It has previously been suggested that azathioprine may increase the rate of resorption by osteoclasts, thus resulting in overall bone loss (Cegiela et al., 2013). Azathioprine was found to cause a reduction in bone mass and mineral substances, as well as a reduction in calcium content which could indicate increased resorption (Cegiela et al., 2013). However, the Ctx levels did not significantly increase in our bone model which would suggest that the effects of azathioprine are not altering osteoclast function. By looking at osteoclast function with azathioprine treatment, it could be determined if azathioprine induces autophagy in osteoclasts as well as determining if azathioprine treatment affects osteoclast function.

Chapter 5: Final discussion

Finally, in order to enable translation to the human condition, the effects of azathioprine could be tested on osteoblasts extracted and cultured from patients undergoing a total hip replacement. Similarly to our preliminary studies, the effect of azathioprine on bone turnover could be analysed by RT-qPCR as well as autophagy marker expression being monitored by western blot or immunofluorescence staining. Furthermore, apoptosis could be measured along with markers of oxidative stress. This would enable determination of how azathioprine would affect human osteoporotic bone cells. Furthermore, genetic and clinical data could be utilised alongside these results to examine whether patients on azathioprine are more susceptible to bone fractures. This would ultimately allow more personalised treatments for patients that may be predisposed to developing osteoporosis. Overall, this could potentially provide a better quality of care for patients with IBD whilst reducing adverse side effects.

References

References

- Abraham, C., & Medzhitov, R. (2011). Interactions between the host innate immune system and microbes in inflammatory bowel disease. *Gastroenterology*, *140*(6), 1729–1737. <https://doi.org/10.1053/j.gastro.2011.02.012>
- Aburto, M. R., Hurlé, J. M., Varela-Nieto, I., & Magariños, M. (2012). Autophagy During Vertebrate Development. *Cells*, *1*(4), 428–448. <https://doi.org/10.3390/cells1030428>
- Agrawal, M., Arora, S., Li, J., Rahmani, R., Sun, L., Steinlauf, A. F., ... Zaidi, M. (2011). Bone, inflammation, and inflammatory bowel disease. *Current Osteoporosis Reports*, *9*(4), 251–257. <https://doi.org/10.1007/s11914-011-0077-9>
- Ali, T., Lam, D., Bronze, M. S., & Humphrey, M. B. (2010). Osteoporosis in Inflammatory Bowel Disease. *Am J Med*, *122*(7), 599–604. <https://doi.org/10.1016/j.amjmed.2009.01.022>.Osteoporosis
- Almeida, M. (2011). Unraveling the role of FoxOs in bone - insights from mouse models. *Bone*, *49*(3), 319–327. <https://doi.org/10.1016/j.bone.2011.05.023>.Unraveling
- Almeida, M., & Brien, C. A. O. (2013). Basic Biology of Skeletal Aging : Role of Stress Response Pathways. *Journal of Gerontology*, *68*(10), 1197–1208. <https://doi.org/10.1093/gerona/glt079>
- Baumgart, D. C., & Carding, S. R. (2007). Inflammatory bowel disease: cause and immunobiology. *Lancet*, *369*(9573), 1627–1640. [https://doi.org/10.1016/S0140-6736\(07\)60750-8](https://doi.org/10.1016/S0140-6736(07)60750-8)
- Bianchi, M. L. (2010). Inflammatory bowel diseases, celiac disease, and bone. *Archives of Biochemistry and Biophysics*, *503*(1), 54–65. <https://doi.org/10.1016/j.abb.2010.06.026>
- Bonewald, L. F. (2011). The amazing osteocyte. *Journal of Bone and Mineral Research*, *26*(2), 229–238. <https://doi.org/10.1002/jbmr.320>
- Brandi, M. L. (2009). Microarchitecture, the key to bone quality. *Rheumatology (United Kingdom)*, *48*(SUPPL.4). <https://doi.org/10.1093/rheumatology/kep273>
- Cegiela, U., Kaczmarczyk-Sedlak, I., Pytlik, M., Folwarczna, J., Nowińska, B., & Fronczek-Sokł, J. (2013). Alendronate prevents development of the skeletal changes induced by azathioprine in rats. *Acta Poloniae Pharmaceutica - Drug Research*, *70*(2), 309–315.
- Chaabane, W., & Appell, M. L. (2016). Interconnections between apoptotic and autophagic pathways during thiopurine-induced toxicity in cancer cells : the role of reactive oxygen species. *Oncotarget*, *7*(46), 75616–75634.
- Chapurlat, R. D., & Confavreux, C. B. (2016). Novel biological markers of bone: From bone metabolism to bone physiology. *Rheumatology (United Kingdom)*, *55*(10), 1714–1725. <https://doi.org/10.1093/rheumatology/kev410>
- Chen, G., Deng, C., & Li, Y. P. (2012). TGF- β and BMP signaling in osteoblast differentiation and bone formation. *International Journal of Biological Sciences*, *8*(2), 272–288. <https://doi.org/10.7150/ijbs.2929>

References

- Chen, K., Hua, Y., Sheng, Y., & Jiang, D. (2014). Decreased activity of osteocyte autophagy with aging may contribute to the bone loss in senile population. *Histochem Cell Biol*, *142*, 285–295. <https://doi.org/10.1007/s00418-014-1194-1>
- Choi, A. M. K., Ryter, S. W., & Levine, B. (2013). Autophagy in Human Health and Disease. *New England Journal of Medicine*, *368*(7), 651–662. <https://doi.org/10.1056/NEJMra1205406>
- Chung, Y., Yoon, S., Choi, B., Hyun, D., Yoon, K., Kim, W., ... Chang, E. (2012). Microtubule-associated protein light chain 3 regulates Cdc42-dependent actin ring formation in osteoclast. *International Journal of Biochemistry and Cell Biology*, *44*(6), 989–997. <https://doi.org/10.1016/j.biocel.2012.03.007>
- Ciuffa, R., Lamark, T., Tarafder, A. K., Guesdon, A., Rybina, S., Hagen, W. J. H., & Johansen, T. (2015). The Selective Autophagy Receptor p62 Forms a Flexible Filamentous Helical Scaffold. *Cell Reports*, *11*(5), 748–758. <https://doi.org/10.1016/j.celrep.2015.03.062>
- Clarke Anderson, H. (2003). Matrix Vesicles and Calcification. *Current Rheumatology Reports*, *5*, 222–226. Retrieved from <https://pdfs.semanticscholar.org/3145/979b4cd3afe4546d60573df500c833bf8ed3.pdf>
- Clowes, J. A., Riggs, B. L., & Khosla, S. (2005). The role of the immune system in the pathophysiology of osteoporosis. *Immunological Reviews*, *208*, 207–227. <https://doi.org/10.1111/j.0105-2896.2005.00334.x>
- Cobo, T., Vilorio, C. G., Solares, L., Fontanil, T., González-Chamorro, E., De Carlos, F., ... Obaya, A. J. (2016). Role of periostin in adhesion and migration of bone remodeling cells. *PLoS ONE*, *11*(1), 1–19. <https://doi.org/10.1371/journal.pone.0147837>
- Compton, J. T., & Lee, F. Y. (2014). Current concepts review: A review of osteocyte function and the emerging importance of sclerostin. *Journal of Bone and Joint Surgery - American Volume*, *96*(19), 1659–1668. <https://doi.org/10.2106/JBJS.M.01096>
- Cosnes, J., Nion-Larmurier, I., Beaugerie, L., Afchain, P., Tiret, E., & Gendre, J. P. (2005). Impact of the increasing use of immunosuppressants in Crohn's disease on the need for intestinal surgery. *Gut*, *237*–241. <https://doi.org/10.1136/gut.2004.045294>
- Czuber-Dochan, W., Ream, E., & Norton, C. (2013). Review article: Description and management of fatigue in inflammatory bowel disease. *Alimentary Pharmacology and Therapeutics*, *37*(5), 505–516. <https://doi.org/10.1111/apt.12205>
- Dallas, S. L., & Bonewald, L. F. (2010). Dynamics of the transition from osteoblast to osteocyte. *Annals of the New York Academy of Sciences*, *1192*(816), 437–443. <https://doi.org/10.1111/j.1749-6632.2009.05246.x>
- Danese, S., Sans, M., & Fiocchi, C. (2004). Inflammatory bowel disease: The role of environmental factors. *Autoimmunity Reviews*, *3*(5), 394–400. <https://doi.org/10.1016/j.autrev.2004.03.002>
- Dart, R. J., & Irving, P. M. (2017). Optimising use of thiopurines in inflammatory bowel disease. *Expert Review of Clinical Immunology*, *13*(9), 877–888. <https://doi.org/10.1080/1744666X.2017.1351298>

References

- Demontis, F., & Perrimon, N. (2010). FOXO/4E-BP Signaling in Drosophila Muscles Regulates Organism-wide Proteostasis During Aging. *Cell*, *143*(5), 813–825. <https://doi.org/10.1016/j.cell.2010.10.007>. FOXO/4E-BP
- Denson, L. (2013). The Role of the Innate and Adaptive Immune System in Pediatric Inflammatory Bowel Disease. *Inflammatory Bowel Diseases*, *19*(9), 2011–2020. <https://doi.org/10.1016/j.dcn.2011.01.002>. The
- Deretic, V., Saitoh, T., & Akira, S. (2013). Autophagy in infection, inflammation, and immunity. *Nat Rev Immunol*, *13*(10), 722–737. <https://doi.org/10.1586/14737175.2015.1028369>. Focused
- DeSelm, C. J., Miller, B. C., Zou, W., Beatty, W. L., van Meel, H., Takahata, Y., ... Virgin, H. W. (2011). Autophagy proteins regulate the secretory component of osteoclastic bone resorption. *Developmental Cell*, *21*(5), 966–974. <https://doi.org/10.1016/j.devcel.2011.08.016>
- Desreumaux, P., & Ghosh, S. (2006). mode of action and delivery of 5-aminosalicylic acid – new evidence. *Alimentary Pharmacology and Therapeutics*, *24*(June), 2–9.
- Diefenbach, K.-A., & Breuer, C.-K. (2006). Pediatric inflammatory bowel disease. *World Journal of Gastroenterology : WJG*, *12*(20), 3204–3212. Retrieved from <http://www.pubmedcentral.nih.gov/articlerender.fcgi?artid=4087963&tool=pmcentrez&rendertype=abstract>
- Dieleman, L. A., Palmen, M. J., Akol, H., Bloemena, E., Peña, A. S., Meuwissen, S. G., & Van Rees, E. P. (1998). Chronic experimental colitis induced by dextran sulphate sodium (DSS) is characterized by Th1 and Th2 cytokines. *Clinical and Experimental Immunology*, *114*, 385–391. Retrieved from http://www.ncbi.nlm.nih.gov/entrez/query.fcgi?db=pubmed&cmd=Retrieve&dopt=AbstractPlus&list_uids=9844047
- Dieren, J. M. Van, Kuipers, E. J., Samsom, J. N., Nieuwenhuis, E. E., & Woude, C. J. Van Der. (2006). Methotrexate , and Mycophenolate Mofetil : Their Mechanisms of Action and Role in the Treatment of IBD. *Inflammatory Bowel Diseases*, *12*(4), 311–327.
- Dobie, R., MacRae, V. E., Pass, C., Milne, E. M., Ahmed, S. F., & Farquharson, C. (2018). Suppressor of cytokine signaling 2 (*Socs2*) deletion protects bone health of mice with DSS-induced inflammatory bowel disease. *Disease Models & Mechanisms*, *11*(1), dmm028456. <https://doi.org/10.1242/dmm.028456>
- Dubinsky, M. C. (2004). Azathioprine, 6-Mercaptopurine in Inflammatory Bowel Disease: Pharmacology, Efficacy, and Safety. *Clinical Gastroenterology and Hepatology*, *2*, 731–743.
- Duran, A., Hernandez, E. D., Reina-campos, M., Karin, M., Diaz-meco, M. T., & Moscat, J. (2016). p62 / SQSTM1 by Binding to Vitamin D Receptor Article p62 / SQSTM1 by Binding to Vitamin D Receptor Inhibits Hepatic Stellate Cell Activity , Fibrosis , and Liver Cancer. *Cancer Cell*, *30*, 595–609. <https://doi.org/10.1016/j.ccell.2016.09.004>
- England, N. (2014). 2013/14 Nhs Standard Contract for Colorectal: Complex Inflammatory Bowel Disease (Adult). *NHS England*, 1–6.
- Farquharson, C., & Staines, K. A. (2011). The skeleton: no bones about it. *Journal of Endocrinology*, *211*, 107–108. <https://doi.org/10.1002/jbmr.306>

References

- Florencio-Silva, R., Rodrigues da Silva, G., de Jesus SIMÕES, M., & Santos SIMÕES, R. (2017a). Osteoporosis and autophagy : What is the relationship ? *Rev. Asso. Médi. Bras*, 63(2), 173–179. <https://doi.org/http://dx.doi.org/10.1590/1806-9282.63.02.173>
- Florencio-Silva, R., Rodrigues da Silva, G., de Jesus SIMÕES, M., & Santos SIMÕES, R. (2017b). Osteoporosis and autophagy : What is the relationship ? *Rev. Asso. Médi. Bras*, 63(2), 173–179. <https://doi.org/http://dx.doi.org/10.1590/1806-9282.63.02.173>
- Florencio-Silva, R., Sasso, G. R. D. S., Sasso-Cerri, E., Simões, M. J., & Cerri, P. S. (2015). Biology of Bone Tissue: Structure, Function, and Factors That Influence Bone Cells. *BioMed Research International*, 2015. <https://doi.org/10.1155/2015/421746>
- Franz-Odendaal, T. A., Hall, B. K., & Witten, P. E. (2006). Buried alive: How osteoblasts become osteocytes. *Developmental Dynamics*, 235(1), 176–190. <https://doi.org/10.1002/dvdy.20603>
- Freeman, H. J. (2014). Natural history and long-term clinical course of Crohn’s disease. *World Journal of Gastroenterology*, 20(1), 31–36. <https://doi.org/10.3748/wjg.v20.i1.31>
- Garnero, P. (2009). Bone markers in osteoporosis. *Current Osteoporosis Reports*, 7(3), 84–90. <https://doi.org/10.1007/s11914-009-0014-3>
- Gaubitz, C., Prouteau, M., Kusmider, B., & Loewith, R. (2016). TORC2 Structure and Function. *Trends in Biochemical Sciences*, 41(6), 532–545. <https://doi.org/10.1016/j.tibs.2016.04.001>
- Gisbert, J. P., Chaparro, M., & Gomollón, F. (2011). Common misconceptions about 5-aminosalicylates and thiopurines in inflammatory bowel disease. *World Journal of Gastroenterology*, 17(30), 3467–3478. <https://doi.org/10.3748/wjg.v17.i30.3467>
- Glick, D., Barth, S., & Macleod, K. F. (2010). Autophagy : cellular and molecular mechanisms. *Journal of Pathology The*, 221(1), 3–12. <https://doi.org/10.1002/path.2697>
- Gupta, N., Lustig, R. H., Chao, C., Vittinghoff, E., Andrews, H., & Leu, C. (2018). Thiopurines are negatively associated with anthropometric parameters in pediatric Crohn’s disease. *World Journal of Gastroenterology*, 24(18), 2036–2046. <https://doi.org/10.3748/wjg.v24.i18.2036>
- Hambli, R., & Hattab, N. (2013). Application of Neural Network and Finite Element Method for Multiscale Prediction of Bone Fatigue crack Growth in Cancellous Bone. *Multiscale Computer Modeling in Biomechanics and Biomedical Engineering*, 14, 3–30. <https://doi.org/10.1007/8415>
- Hamdani, G., Gabet, Y., Rachmilewitz, D., Karmeli, F., Bab, I., & Dresner-Pollak, R. (2008). Dextran sodium sulfate-induced colitis causes rapid bone loss in mice. *Bone*, 43(5), 945–950. <https://doi.org/10.1016/j.bone.2008.06.018>
- Hampe, J., Franke, A., Rosenstiel, P., Till, A., Teuber, M., Huse, K., ... Schreiber, S. (2007). A genome-wide association scan of nonsynonymous SNPs identifies a susceptibility variant for Crohn disease in ATG16L1. *Nature Genetics*, 39(2), 207–212. <https://doi.org/10.1038/ng1954>

References

- Hanauer, S. B. (2004). Review article : aminosalicylates in inflammatory bowel disease. *Aliment Pharmacol Ther*, 20, 60–65.
- Harris, L., Senagore, P., Young, V. B., & McCabe, L. R. (2009). Inflammatory bowel disease causes reversible suppression of osteoblast and chondrocyte function in mice. *AJP: Gastrointestinal and Liver Physiology*, 296(5), G1020–G1029. <https://doi.org/10.1152/ajpgi.90696.2008>
- He, C., & Klionsky, D. J. (2009). Regulation Mechanisms and Signalling Pathways of Autophagy. *Annual Review of Genetics*, 43(68), 67. <https://doi.org/10.1146/annurev-genet-102808-114910.Regulation>
- Head., K., & Jurenka., J. (2003). Inflammatory Bowel Disease Part I: Ulcerative Colitis Pathophysiology and Conventional and Alternative Treatment Options Kathleen. *Ulcerative Colitis*, 8(9). <https://doi.org/10.3109/09637485809142520>
- Henderson, P., Hansen, R., Cameron, F. L., Gerasimidis, K., Rogers, P., Bisset, W. M., Wilson, D. C. (2012). Rising incidence of pediatric inflammatory bowel disease in Scotland. *Inflammatory Bowel Diseases*, 18(6), 999–1005. <https://doi.org/10.1002/ibd.21797>
- Henderson, P., & Stevens, C. (2012). The Role of Autophagy in Crohn's Disease. *Cells*, 1(4), 492–519. <https://doi.org/10.3390/cells1030492>
- Hocking, L. J., Whitehouse, C., & Helfrich, M. H. (2012). Autophagy: A new player in skeletal maintenance? *Journal of Bone and Mineral Research*, 27(7), 1439–1447. <https://doi.org/10.1002/jbmr.1668>
- Hooper, K. M., Barlow, P. G., Stevens, C., & Henderson, P. (2017). Inflammatory bowel disease drugs: A focus on autophagy. *Journal of Crohn's and Colitis*, 11(1), 118–127. <https://doi.org/10.1093/ecco-jcc/jjw127>
- Hurley, J. H., & Schulman, B. A. (2014). Atomistic autophagy: The structures of cellular self-digestion. *Cell*, 157(2), 300–311. <https://doi.org/10.1016/j.cell.2014.01.070>
- Hyams, J., Crandall, W., Kugathasan, S., Griffiths, A., Olson, A., Johanns, J., ... Baldassano, R. (2007). Induction and Maintenance Infliximab Therapy for the Treatment of Moderate-to-Severe Crohn's Disease in Children. *Gastroenterology*, 132, 863–873. <https://doi.org/10.1053/j.gastro.2006.12.003>
- Iida, T., Onodera, K., & Nakase, H. (2017). Role of autophagy in the pathogenesis of inflammatory bowel disease. *World Journal of Gastroenterology*, 23(11), 1944–1953. <https://doi.org/10.3748/wjg.v23.i11.1944>
- Iii, S. J. C., Kulich, S. M., Uechi, G., Balasubramani, M., Mountzouris, J., Day, B. W., & Chu, C. T. (2010). Regulation of the autophagy protein LC3 by phosphorylation. *Journal of Cell Biology*, 190(4), 533–539. <https://doi.org/10.1083/jcb.201002108>
- Iriarte Rodríguez, R., Pulido, S., Rodríguez-de la Rosa, L., Magariños, M., & Varela-Nieto, I. (2015). Age-regulated function of autophagy in the mouse inner ear. *Hearing Research*, 330, 39–50. <https://doi.org/10.1016/j.heares.2015.07.020>
- Itakura, E., & Mizushima, N. (2011). p62 targeting to the autophagosome formation site requires self-oligomerization but not LC3 binding. *Journal of Cell Biology*, 192(1), 17–27. <https://doi.org/10.1083/jcb.201009067>
- Jacobs, C. R. (2000). Mechanobiology of cancellous bone structural adaptation. *Journal*

References

- of Rehabilitation Research and Development*, 37(2), 209–216.
- Jian, W. L., & Bao, L. J. (2012). Microautophagy: lesser-known self-eating. *Cellular and Molecular Life Sciences*, 69, 1125–1136. <https://doi.org/10.1007/s00018-011-0865-5>
- Jo, E. (2013). Autophagy as an innate defense against mycobacteria. *Pathogens and Diseases*, 67, 108–118. <https://doi.org/10.1111/2049-632X.12023>
- Jung, Y., Song, J., Shiozawa, Y., Wang, J., Wang, Z., Williams, B., Taichman, R. S. (2008). Hematopoietic Stem Cells Regulate Mesenchymal Stromal Cell Induction into Osteoblasts Thereby Participating in The Formation of the Stem Cell Niche. *Stem Cells*, 26(8), 2042–2051. <https://doi.org/10.5935/1984-6835.20140101>
- Kang, H., Lee, J., Kim, M., Hwan, Y., & Jung, J. (2018). Genome-wide identification of 99 autophagy-related (Atg) genes in the monogonont rotifer *Brachionus* spp . and transcriptional modulation in response to cadmium. *Aquatic Toxicology*, 201(April), 73–82. <https://doi.org/10.1016/j.aquatox.2018.05.021>
- Kanzaki, H., Chiba, M., Shimizu, Y., & Mitani, H. (2002). Periodontal Ligament Cells Under Mechanical Stress Induce Osteoclastogenesis by Receptor Activator of Nuclear Factor B Ligand Up-Regulation via Prostaglandin E2 Synthesis. *Journal of Bone and Mineral Research*, 17(2), 210–220.
- Kaser, A., Zeissig, S., & Blumberg, R. S. (2010). Inflammatory Bowel Disease. *Annual Review Immunology*, 28, 573–621. <https://doi.org/10.1146/annurev-immunol-030409-101225.Inflammatory>
- Kim, J. H., & Kim, N. (2016). Signaling Pathways in Osteoclast Differentiation. *Chonnam Medical Journal*, 52(1), 12. <https://doi.org/10.4068/cmj.2016.52.1.12>
- Kim, J., Kim, Y. C., Fang, C., Russell, R. C., Kim, J. H., Fan, W., & Liu, R. (2012). Differential Regulation of Distinct Vps34 Complexes by AMPK in Nutrient Stress and Autophagy. *Cell*, 152(1–2), 290–303. <https://doi.org/10.1016/j.cell.2012.12.016>
- Kim, M. S., Day, C. J., Selinger, C. I., Magno, C. L., Stephens, R. J., & Morrison, N. A. (2006). MCP-1-induced Human Osteoclast-like Cells Are Tartrate-resistant Acid Phosphatase , NFATc1 , and Calcitonin Receptor-positive but Require Receptor Activator of NF κ B Ligand for Bone Resorption *. *Journal of Biological Chemistry*, 281(2), 1274–1285. <https://doi.org/10.1074/jbc.M510156200>
- King, J. S., Veltman, D. M., Insall, R. H., King, J. S., Veltman, D. M., & Insall, R. H. (2011). The induction of autophagy by mechanical stress. *Autophagy*, 7(12), 1490–1499. <https://doi.org/10.4161/auto.7.12.17924>
- Klionsky, D. J., & Codogno, P. (2013). The mechanism and physiological function of macroautophagy. *Journal of Innate Immunity*, 5(5), 427–433. <https://doi.org/10.1159/000351979>
- Knights, D., Lassen, K. G., & Xavier, R. J. (2013). Advances in inflammatory bowel disease pathogenesis: Linking host genetics and the microbiome. *Gut*, 62(10), 1505–1510. <https://doi.org/10.1136/gutjnl-2012-303954>
- Kohr, B., Gardet, A., & Xavier, R. J. (2011). Genetics and pathogenesis of inflammatory bowel disease. *Nature*, 474(7351), 307–317. <https://doi.org/10.1038/nature10209.Genetics>

References

- Komori, T. (2006). Regulation of osteoblast differentiation by transcription factors. *Journal of Cellular Biochemistry*, 99(5), 1233–1239. <https://doi.org/10.1002/jcb.20958>
- Kostik, M. M., Smirnov, A. M., Demin, G. S., Mnuskina, M. M., Scheplyagina, L. A., & Larionova, V. I. (2013). Genetic polymorphisms of collagen type I $\alpha 1$ chain (COL1A1) gene increase the frequency of low bone mineral density in the subgroup of children with juvenile idiopathic arthritis. *EPMA Journal*, 4(1), 15. <https://doi.org/10.1186/1878-5085-4-15>
- Kucharzik, T., Maaser, C., Lügering, A., Kagnoff, M., Mayer, L., Targan, S., & Domschke, W. (2006). Recent understanding of IBD pathogenesis: Implications for future therapies. *Inflammatory Bowel Diseases*, 12(11), 1068–1082. <https://doi.org/10.1097/01.mib.0000235827.21778.d5>
- Kuma, A., Komatsu, M., & Mizushima, N. (2017). Autophagy-monitoring and autophagy-deficient mice. *Autophagy*, 13(10), 1619–1628. <https://doi.org/10.1080/15548627.2017.1343770>
- Kuma, A., Matsui, M., & Mizushima, N. (2007). LC3, an autophagosome marker, can be incorporated into protein aggregates independent of autophagy: Caution in the interpretation of LC3 localization. *Autophagy*, 3(4), 323–328. <https://doi.org/10.4161/auto.4012>
- Lamark, T., Kirkin, V., Dikic, I., & Johansen, T. (2009). NBR1 and p62 as cargo receptors for selective autophagy of ubiquitinated targets. *Cell Cycle*, 8(13), 1986–1990. <https://doi.org/10.4161/cc.8.13.8892>
- Langholz, E. (2010). Current trends in inflammatory bowel disease: The natural history. *Therapeutic Advances in Gastroenterology*, 3(2), 77–86. <https://doi.org/10.1177/1756283X10361304>
- Lee, K.-W., Yook, J.-Y., Son, M.-Y., Kim, M.-J., Koo, D.-B., Han, Y.-M., & Cho, Y. S. (2010). Rapamycin Promotes the Osteoblastic Differentiation of Human Embryonic Stem Cells by Blocking the mTOR Pathway and Stimulating the BMP/Smad Pathway. *Stem Cells and Development*, 19(4), 557–568. <https://doi.org/10.1089/scd.2009.0147>
- Li, X., Chang, B., Wang, B., Bu, W., Zhao, L., Liu, J., ... Sun, H. (2017). Rapamycin promotes osteogenesis under inflammatory conditions. *Molecular Medicine Reports*, 16(6), 8923–8929. <https://doi.org/10.3892/mmr.2017.7693>
- Lichtenstein, G. R. (2006). American Gastroenterological Association Institute Technical Review on Corticosteroids, Immunomodulators, and Infliximab in Inflammatory Bowel Disease. *Gastroenterology*, 130, 940–987. <https://doi.org/10.1016/j.gastro.2006.01.048>
- Lilienbaum, A. (2013). Relationship between the proteasomal system and autophagy. *Biochem Mol Bio*, 4(1), 1–26.
- Livak, K. J., & Schmittgen, T. D. (2001). Analysis of Relative Gene Expression Data Using Real-Time Quantitative PCR and the $2^{-\Delta\Delta CT}$ Method. *Methods*, 25, 402–408. <https://doi.org/10.1006/meth.2001.1262>
- Mackie, E. J., Tatarczuch, L., & Mirams, M. (2011). The skeleton: A multi-functional complex organ. The growth plate chondrocyte and endochondral ossification. *Journal of Endocrinology*, 211(2), 109–121. <https://doi.org/10.1530/JOE-11-0048>

References

- Maconi, G., Ardizzone, S., Cucino, C., Bezzio, C., Russo, A. G., & Porro, G. B. (2010). Pre-illness changes in dietary habits and diet as a risk factor for inflammatory bowel disease: A case-control study. *World Journal of Gastroenterology*, *16*(34), 4297–4304. <https://doi.org/10.3748/wjg.v16.i34.4297>
- Manolagas SC. (2000). Birth and death of bone cells: basic regulatory mechanisms and implications for the pathogenesis and treatment of osteoporosis. *Endocrine Reviews*, *21*(January), 115–137. <https://doi.org/10.1210/edrv.21.2.0395>
- Marcuzzi., A., Bianco., A. ., Girardelli., M., Tommasini., A., Martellosi., S., & Monasta., L. (2013). Genetic and functional profiling of Crohn's disease: Autophagy mechanism and susceptibility to infectious diseases. *BioMed Research International*, *2013*, 297501. <https://doi.org/http://dx.doi.org/10.1155/2013/297501>
- Markowitz, J. (2008). Current treatment of inflammatory bowel disease in children. *Digestive and Liver Disease*, *40*(1), 16–21. <https://doi.org/10.1016/j.dld.2007.07.167>
- Mckee-muir, O. C., & Russell, R. C. (2017). *Mechanistic Target of Rapamycin: The Alpha and Omega of Autophagy Regulation. Autophagy: Cancer, Other Pathologies, Inflammation, Immunity, Infection, and Aging* (Vol. 12). Elsevier Inc. <https://doi.org/10.1016/B978-0-12-812146-7.00009-3>
- McSorley, S. J., & Bevins, C. L. (2013). Paneth cells: Targets of friendly fire. *Nature Immunology*, *14*(2), 114–116. <https://doi.org/10.1038/ni.2519>
- Miznerova, E., Hlavaty, T., Koller, T., Toth, J., Holociova, K., Huorka, M., ... Payer, J. (2013). The prevalence and risk factors for osteoporosis in patients with inflammatory bowel disease Miznerova. *Bratislavské Lekárske Listy*, *114*(8), 439–445. <https://doi.org/10.4149/BLL>
- Moriceau, G., Ory, B., Mitrofan, L., Riganti, C., Blanchard, F., Brion, R., ... Heymann, D. (2010). Zoledronic acid potentiates mTOR inhibition and abolishes the resistance of osteosarcoma cells to RAD001 (Everolimus): pivotal role of the prenylation process Gatién. *Cancer Research*, *70*(24), 10329–10339. <https://doi.org/10.1016/j.dcn.2011.01.002>.The
- Moss, A. C., & Farrell, R. J. (2006). Infliximab for induction and maintenance therapy for ulcerative colitis. *Gastroenterology*, *131*(5), 1649–1651. <https://doi.org/10.1053/j.gastro.2006.09.039>
- Nakashima, T., Hayashi, M., Fukunaga, T., Kurata, K., Oh-Hora, M., Feng, J. Q., ... Takayanagi, H. (2011). Evidence for osteocyte regulation of bone homeostasis through RANKL expression. *Nature Medicine*, *17*(10), 1231–1234. <https://doi.org/10.1038/nm.2452>
- Nishida, A., Inoue, R., Inatomi, O., Bamba, S., Naito, Y., & Andoh, A. (2017). Gut microbiota in the pathogenesis of inflammatory bowel disease. *Clinical Journal of Gastroenterology*, *11*(1), 1–10. <https://doi.org/10.1007/s12328-017-0813-5>
- Nollet, M., Santucci-Darmanin, S., Breuil, V., Al-Sahlane, R., Cros, C., Topi, M., ... Pierrefite-Carle, V. (2014). Autophagy in osteoblasts is involved in mineralization and bone homeostasis. *Autophagy*, *10*(11), 1965–1977. <https://doi.org/10.4161/auto.36182>
- Nudelman, F., Pieterse, K., George, A., Bomans, P. H. H., Friedrich, H., Brylka, L. J., ... Sommerdijk, N. A. J. M. (2010). The role of collagen in bone apatite formation

References

- in the presence of hydroxyapatite nucleation inhibitors. *Nature Materials*, 9(12), 1004–1009. <https://doi.org/10.1038/nmat2875>
- Nuschke, A., Rodrigues, M., Stolz, D. B., Chu, C. T., Griffith, L., & Wells, A. (2014). Human mesenchymal stem cells / multipotent stromal cells consume accumulated autophagosomes early in differentiation. *Stem Cell Research & Therapy*, 5, 1–14.
- Olszta, M. J., Cheng, X., Jee, S. S., Kumar, R., Kim, Y. Y., Kaufman, M. J., ... Gower, L. B. (2007). Bone structure and formation: A new perspective. *Materials Science and Engineering R: Reports*, 58(3–5), 77–116. <https://doi.org/10.1016/j.mser.2007.05.001>
- Onal, M., Piemontese, M., Xiong, J., Wang, Y., Han, L., Ye, S., ... O'Brien, C. A. (2013). Suppression of autophagy in osteocytes mimics skeletal aging. *Journal of Biological Chemistry*, 288(24), 17432–17440. <https://doi.org/10.1074/jbc.M112.444190>
- Orenstein, S. J., & Cuervo, A. M. (2010). Chaperone-mediated autophagy: Molecular mechanisms and physiological relevance. *Semin Cell Dev Biol*, 21(7), 719–726. <https://doi.org/10.1016/j.semcdb.2010.02.005>.Chaperone-mediated
- Parkes, M., Barrett, J. C., Prescott, N., Tremelling, M., Carl, A., Fisher, S. A., ... Forbes, A. (2007). Sequence variants in the autophagy gene IRGM and multiple other replicating loci contribute to Crohn disease susceptibility. *Nat. Genet.*, 39(7), 830–832. <https://doi.org/10.1038/ng2061>.Sequence
- Pierrefite-Carle, V., Santucci-Darmanin, S., Breuil, V., Camuzard, O., & Carle, G. F. (2015). Autophagy in bone: Self-eating to stay in balance. *Ageing Research Reviews*, 24, 206–217. <https://doi.org/10.1016/j.arr.2015.08.004>
- Pithadia, A. B., & Jain, S. (2011). Treatment of inflammatory bowel disease (IBD). *Pharmacological Reports*, 63(3), 629–642. [https://doi.org/10.1016/S1734-1140\(11\)70575-8](https://doi.org/10.1016/S1734-1140(11)70575-8)
- Qian, M., Fang, X., & Wang, X. (2017). Autophagy and inflammation. *Clinical and Translational Medicine*, 6(1), 24. <https://doi.org/10.1186/s40169-017-0154-5>
- Qian, X., Li, X., Cai, Q., Zhang, C., Yu, Q., Jiang, Y., ... Lu, Z. (2017). Phosphoglycerate Kinase 1 Phosphorylates Beclin1 to Induce Autophagy. *Molecular Cell*, 65(5), 917–931.e6. <https://doi.org/10.1016/j.molcel.2017.01.027>
- Raggatt, L. J., & Partridge, N. C. (2010). Cellular and molecular mechanisms of bone remodeling. *Journal of Biological Chemistry*, 285(33), 25103–25108. <https://doi.org/10.1074/jbc.R109.041087>
- Razzaque, M. S. (2011). Osteocalcin: A pivotal mediator or an innocent bystander in energy metabolism? *Nephrology Dialysis Transplantation*, 26(1), 42–45. <https://doi.org/10.1093/ndt/gfq721>
- Rios, H., Koushik, S. V., Wang, H., Wang, J., Zhou, H.-M., Lindsley, A., ... Conway, S. J. (2005). periostin Null Mice Exhibit Dwarfism, Incisor Enamel Defects, and an Early-Onset Periodontal Disease-Like Phenotype. *Molecular and Cellular Biology*, 25(24), 11131–11144. <https://doi.org/10.1128/MCB.25.24.11131-11144.2005>
- Rufini, S., Ciccacci, C., Di Fusco, D., Ruffa, A., Pallone, F., Novelli, G., ... Borgiani, P. (2015). Autophagy and inflammatory bowel disease: Association between variants of the autophagy-related IRGM gene and susceptibility to Crohn's disease.

References

- Digestive and Liver Disease*, 47(9), 744–750.
<https://doi.org/10.1016/j.dld.2015.05.012>
- Rutkovskiy, A., Stenslkken, K.-O., & Vaage, I. J. (2016). Osteoblast Differentiation at a Glance. *Medical Science Monitor Basic Research*, 22, 95–106.
<https://doi.org/10.12659/MSMBR.901142>
- Sambrook, P., & Cooper, C. (2010). Osteoporosis. *Lancet*, 367, 2010–2018.
- Schulte, C. M. S., Dignass, A. U., Goebell, H., Roher, H. D., & Schulte, K. M. (2000). Genetic factors determine extent of bone loss in inflammatory bowel disease. *Gastroenterology*, 119(4), 909–920. <https://doi.org/10.1053/gast.2000.18158>
- Shapiro, F. (2008). Bone development and its relation to fracture repair. The role of mesenchymal osteoblasts and surface osteoblasts. *European Cells and Materials*, 15, 53–76. <https://doi.org/10.22203/eCM.v015a05>
- Shapiro, I. M., Layfield, R., Lotz, M., Settembre, C., & Whitehouse, C. (2014). Boning up on autophagy :The role of autophagy in skeletal biology. *Autophagy*, 10(1), 7–19. <https://doi.org/10.4161/auto.26679>
- Shaw, S. Y., Blanchard, J. F., & Bernstein, C. N. (2010). Association between the use of antibiotics in the first year of life and pediatric inflammatory bowel disease. *American Journal of Gastroenterology*, 105(12), 2687–2692.
<https://doi.org/10.1038/ajg.2010.398>
- Shen, F. (2004). Cytokines link osteoblasts and inflammation: microarray analysis of interleukin-17- and TNF- -induced genes in bone cells. *Journal of Leukocyte Biology*, 77(3), 388–399. <https://doi.org/10.1189/jlb.0904490>
- Shen, G., Ren, H., Qiu, T., Zhang, Z., Zhao, W., Yu, X., ... Jiang, X. (2018). *Mammalian target of rapamycin as a therapeutic target in osteoporosis*. *Journal of Cellular Physiology* (Vol. 233). <https://doi.org/10.1002/jcp.26161>
- Shih, D. Q., Targan, S. R., & McGovern, D. (2008). Recent Advances in IBD Pathogenesis: Genetics and Immunobiology. *Current Gastroenterology*, 10(6), 568–575. <https://doi.org/10.1016/j.neuroimage.2013.08.045>.The
- Singha, U. K., Jiang, Y., Yu, S., Luo, M., Lu, Y., Zhang, J., & Xiao, G. (2008). Rapamycin inhibits osteoblast proliferation and differentiation in MC3T3-E1 cells and primary mouse bone marrow stromal cells. *Journal of Cellular Biochemistry*, 103(2), 434–446. <https://doi.org/10.1002/jcb.21411>
- Sommerfeldt, D., & Rubin, C. (2001). Biology of bone and how it orchestrates the form and function of the skeleton. *European Spine Journal*, 10(SUPPL. 2), 86–95.
<https://doi.org/10.1007/s005860100283>
- Song, C., Song, C., & Tong, F. A. N. (2014). Autophagy induction is a survival response against oxidative stress in bone marrow e derived mesenchymal stromal cells. *Journal of Cytotherapy*, 16(10), 1361–1370.
<https://doi.org/10.1016/j.jcyt.2014.04.006>
- Staines, K. A., MacRae, V. E., & Farquharson, C. (2012). The importance of the SIBLING family of proteins on skeletal mineralisation and bone remodelling. *Journal of Endocrinology*, 214(3), 241–255. <https://doi.org/10.1530/JOE-12-0143>
- Staines, K., Zhu, D., Farquharson, C., & MacRae, V. E. (2014). Identification of novel regulators of osteoblast matrix mineralization by time series transcriptional

References

- profiling. *Journal of Bone and Mineral Metabolism*, 32(3), 240–251.
<https://doi.org/10.1007/s00774-013-0493-2>
- Stocco, G., Cuzzoni, E., Iudicibus, S. De, Favretto, D., Malusà, N., Martellosi, S., ... Martellosi, S. (2015). Thiopurine metabolites variations during co-treatment with aminosalicylates for inflammatory bowel disease : Effect of N-acetyl transferase polymorphisms. *World Journal of Gastroenterology*, 21(12), 3571–3578.
<https://doi.org/10.3748/wjg.v21.i12.3571>
- Sylvester, F. A., & Vella, A. T. (2016). Inflammatory Bowel Disease and Bone. *Osteoimmunology*, 271–281. <https://doi.org/10.1016/B978-0-12-800571-2.00015-3>
- Tsampalieros, A., Griffiths, A. M., Barrowman, N., & MacK, D. R. (2011). Use of C-reactive protein in children with newly diagnosed inflammatory bowel disease. *Journal of Pediatrics*, 159(2), 340–342.
<https://doi.org/10.1016/j.jpeds.2011.04.028>
- Väänänen, H. K., & Laitala-Leinonen, T. (2008). Osteoclast lineage and function. *Archives of Biochemistry and Biophysics*, 473(2), 132–138.
<https://doi.org/10.1016/j.abb.2008.03.037>
- Van Dijk, F. S., Huizer, M., Kariminejad, A., Marcelis, C. L., Plomp, A. S., Terhal, P. A., ... Pals, G. (2010). Complete COL1A1 allele deletions in osteogenesis imperfecta. *Genetics in Medicine*, 12(11), 736–741.
<https://doi.org/10.1097/GIM.0b013e3181f01617>
- Vestergaard, P., Rejnmark, L., & Mosekilde, L. (2006). Methotrexate, azathioprine, cyclosporine, and risk of fracture. *Calcified Tissue International*, 79(2), 69–75.
<https://doi.org/10.1007/s00223-006-0060-0>
- Vinod, V., Padmakrishnan, C. J., Vijayan, B., & Gopala, S. (2014). How can i halt thee? the puzzles involved in autophagic inhibition. *Pharmacological Research*, 82, 1–8.
<https://doi.org/10.1016/j.phrs.2014.03.005>
- Waljee, A. K., Wiitala, W. L., Govani, S., Stidham, R., Saini, S., Hou, J., ... Higgins, P. D. R. (2016). Corticosteroid Use and Complications in a US Inflammatory Bowel Disease Cohort. *PloS One*, 11(6), 1–14.
<https://doi.org/10.1371/journal.pone.0158017>
- Wang, K., Niu, J., Kim, H., & Kolattukudy, P. E. (2011). Osteoclast precursor differentiation by MCP1P via oxidative stress , endoplasmic reticulum stress , and autophagy. *Journal of Molecular Cell Biology*, 3, 360–368.
- Warner, B., Johnston, E., Arenas-Hernandez, M., Marinaki, A., Irving, P., & Sanderson, J. (2018). A practical guide to thiopurine prescribing and monitoring in IBD. *Frontline Gastroenterology*, 9(1), 10–15. <https://doi.org/10.1136/flgastro-2016-100738>
- Waters, S., Marchbank, K., Solomon, E., Whitehouse, C., & Gautel, M. (2009). Interactions with LC3 and polyubiquitin chains link nbr1 to autophagic protein turnover. *FEBS*, 583(12), 1846–1852. <https://doi.org/10.1016/j.febslet.2009.04.049>
- Weinstein, R. S., & Manolagas, S. C. (2000). Apoptosis and osteoporosis. *American Journal of Medicine*, 108(2), 153–164. [https://doi.org/10.1016/S0002-9343\(99\)00420-9](https://doi.org/10.1016/S0002-9343(99)00420-9)
- Whitehouse, C. A., Waters, S., Marchbank, K., Horner, A., McGowan, N. W. A.,

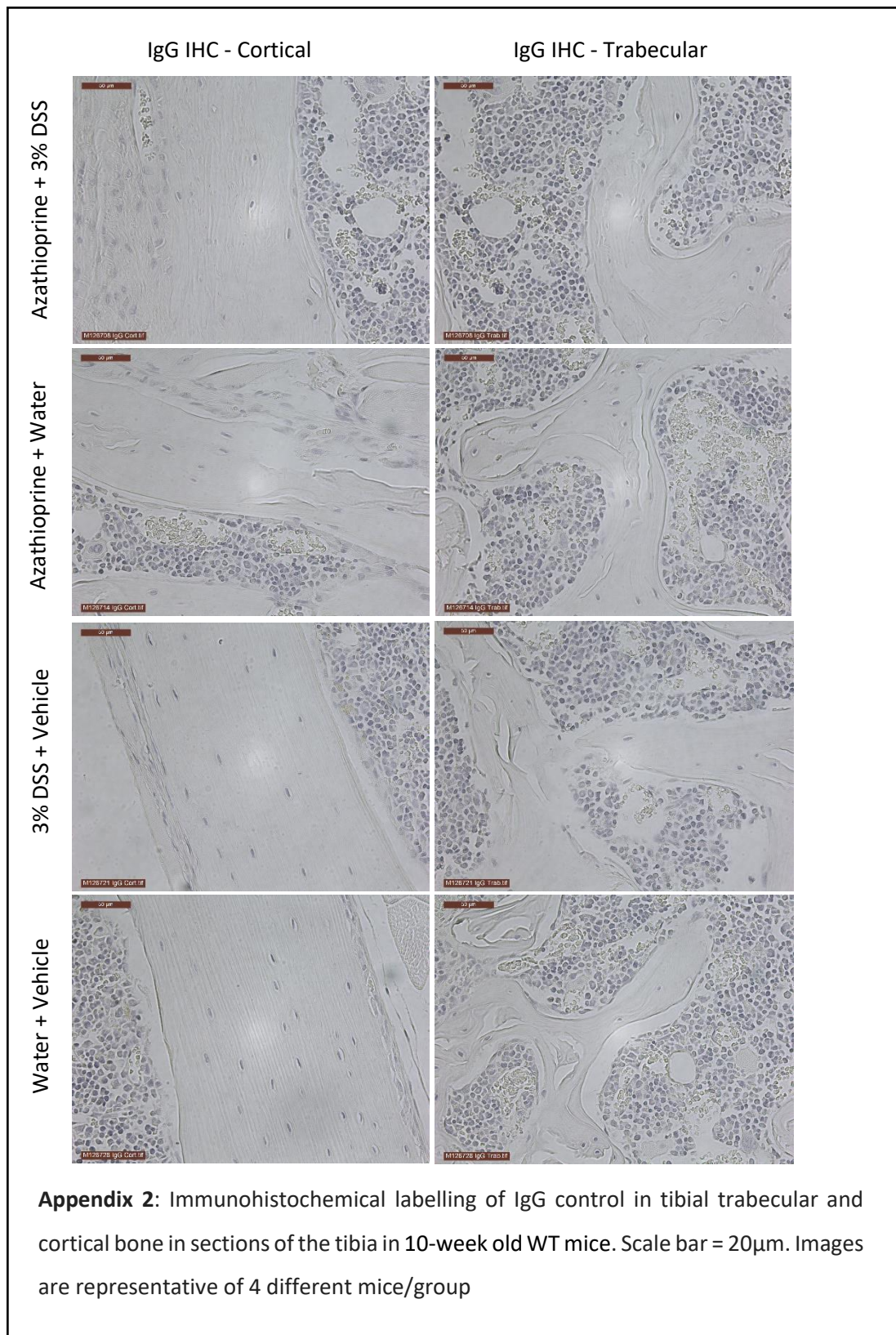
References

- Jovanovic, J. V., Solomon, E. (2010). Neighbor of Brca1 gene (Nbr1) functions as a negative regulator of postnatal osteoblastic bone formation and p38 MAPK activity. *PNAS*, *107*(29), 12913–12918. <https://doi.org/10.1073/pnas.0913058107>
- Xia, X., Kar, R., Gluhak-heinrich, J., Yao, W., Lane, N. E., Bonewald, L. F., Jiang, J. X. (2010). Glucocorticoid-Induced Autophagy in Osteocytes. *Journal of Bone and Mineral Metabolism*, *25*(11), 2479–2488. <https://doi.org/10.1002/jbmr.160>
- Xiong, J., Onal, M., Jilka, R. L., Weinstein, R. S., Manolagas, S. C., & Brien, C. A. O. (2012). Matrix-embedded cells control osteoclast formation. *Nat Med*, *17*(10), 1235–1241. <https://doi.org/10.1038/nm.2448.Matrix-embedded>
- Xiu, Y., Xing, L., Boyce, B. F., Xiu, Y., Xu, H., Zhao, C., Yao, Z. (2014). Chloroquine reduces osteoclastogenesis in murine osteoporosis by preventing TRAF3 degradation. *The Journal of Clinical Investigation*, *124*(1), 297–310. <https://doi.org/10.1172/JCI66947.double-KO>
- Yamamoto, A., Tagawa, Y., Yoshimori, T., Moriyama, Y., Masaki, R., & Tashiro, Y. (1998). Bafilomycin Ai Prevents Maturation of Autophagic Vacuoles by Inhibiting H-4-II-E between Autophagosomes and Lysosomes in Rat Hepatoma Cell Line, H-4-II-E cells. *Cell Structure and Function*, *23*, 33–42. <https://doi.org/10.1247/csf.23.33>
- Yao, W., Dai, W., Jiang, L., Zhong, Z., Ritchie, R. O., Li, X., Oaks, T. (2016). Sclerostin-antibody treatment of glucocorticoid-induced osteoporosis maintained bone mass and strength. *Osteoporos Int*, *27*(1), 283–294. <https://doi.org/10.1007/s00198-015-3308-6>
- Yu, L., Chen, Y., & Tooze, S. A. (2017). Autophagy pathway: cellular and molecular mechanisms. *Autophagy*, *8627*, 00–00. <https://doi.org/10.1080/15548627.2017.1378838>
- Zahm, A. M., Bohensky, J., Adams, C. S., Shapiro, I. M., & Srinivas, V. (2011). Bone cell autophagy is regulated by environmental factors. *Cells Tissues Organs*, *194*(2–4), 274–278. <https://doi.org/10.1159/000324647>
- Zhang, Y. Z., & Li, Y. Y. (2014). Inflammatory bowel disease: Pathogenesis. *World Journal of Gastroenterology*, *20*(1), 91–99. <https://doi.org/10.3748/wjg.v20.i1.91>

Appendix

Appendix Table 1: Significance of weight changes between treatment groups of mice in DSS-study taken daily over the 18-day treatment period. Differences between treatment groups were assessed by two-way analysis of variance (ANOVA) for which tests for multiple comparisons were conducted. Bonferroni tests were carried out to correct for multiple testing between groups.

	Groups	Significance	P value
Day 5	Water + vehicle vs. 3% DSS + vehicle	**	0.0011
	Water + vehicle vs. 3% DSS + Azathioprine	***	0.0006
	Water + Azathioprine vs. 3% DSS + Azathioprine	*	0.0384
Day 6	Water + vehicle vs. 3% DSS + vehicle	****	<0.0001
	Water + vehicle vs. 3% DSS + Azathioprine	****	<0.0001
	3% DSS + vehicle vs. Water + Azathioprine	***	0.0001
	Water + Azathioprine vs. 3% DSS + Azathioprine	****	<0.0001
Day 7	Water + vehicle vs. 3% DSS + vehicle	****	<0.0001
	Water + vehicle vs. 3% DSS + Azathioprine	****	<0.0001
	3% DSS + vehicle vs. Water + Azathioprine	***	0.0001
	Water + Azathioprine vs. 3% DSS + Azathioprine	****	<0.0001
Day 8	Water + vehicle vs. 3% DSS + vehicle	***	0.0001
	Water + vehicle vs. 3% DSS + Azathioprine	****	<0.0001
	Water + Azathioprine vs. 3% DSS + Azathioprine	***	0.0006
Day 9	Water + vehicle vs. 3% DSS + vehicle	**	0.0013
	Water + vehicle vs. 3% DSS + Azathioprine	****	<0.0001
Day 10	Water + vehicle vs. 3% DSS + vehicle	*	0.0267
	Water + vehicle vs. 3% DSS + Azathioprine	**	0.0051
Day 11	Water + vehicle vs. 3% DSS + vehicle	*	0.0195
	Water + vehicle vs. 3% DSS + Azathioprine	*	0.0256
Day 12	Water + vehicle vs. 3% DSS + vehicle	**	0.0033
	Water + vehicle vs. Water + Azathioprine	*	0.0158
	Water + vehicle vs. 3% DSS + Azathioprine	***	0.0008
Day 13	Water + vehicle vs. 3% DSS + vehicle	***	0.001
	Water + vehicle vs. Water + Azathioprine	**	0.002
	Water + vehicle vs. 3% DSS + Azathioprine	****	<0.0001
Day 14	Water + vehicle vs. 3% DSS + vehicle	**	0.0067
	Water + vehicle vs. Water + Azathioprine	**	0.0028
	Water + vehicle vs. 3% DSS + Azathioprine	***	0.0001
Day 15	Water + vehicle vs. 3% DSS + vehicle	***	0.0007
	Water + vehicle vs. Water + Azathioprine	***	0.0001
	Water + vehicle vs. 3% DSS + Azathioprine	****	<0.0001
Day 16	Water + vehicle vs. 3% DSS + vehicle	*	0.0105
	Water + vehicle vs. Water + Azathioprine	**	0.0059
	Water + vehicle vs. 3% DSS + Azathioprine	****	<0.0001
Day 17	Water + vehicle vs. 3% DSS + vehicle	**	0.0045
	Water + vehicle vs. Water + Azathioprine	***	0.0003
	Water + vehicle vs. 3% DSS + Azathioprine	****	<0.0001
Day 18	Water + vehicle vs. 3% DSS + vehicle	***	0.0001
	Water + vehicle vs. Water + Azathioprine	****	<0.0001
	Water + vehicle vs. 3% DSS + Azathioprine	****	<0.0001



Appendix 2: Immunohistochemical labelling of IgG control in tibial trabecular and cortical bone in sections of the tibia in 10-week old WT mice. Scale bar = 20μm. Images are representative of 4 different mice/group